Natural Resources Canada | Ressources naturelles Canada

GEOLOGICAL SURVEY OF CANADA
PREPRINT 5

Quaternary geology of the south Core Zone area, Quebec and Labrador

J.M. Rice, R.C. Paulen, M. Ross, M.B. McClenaghan, and H.E. Campbell

2022

Canada

GEOLOGICAL SURVEY OF CANADA
PREPRINT 5

Quaternary geology of the south Core Zone area, Quebec and Labrador

J.M. Rice[1*], R.C. Paulen[1], M. Ross[2], M.B. McClenaghan[1], and H.E Campbell[3]

[1*]Geological Survey of Canada, 601 Booth Street, Ottawa, Ontario
[2]University of Waterloo, 200 University Avenue West, Waterloo, Ontario
[3]Newfoundland and Labrador Geological Survey, 50 Elizabeth Avenue, St. John's, Newfoundland and Labrador
*Corresponding author: jessey.rice@nrcan-rncan.gc.ca

2022

Permanent link: https://doi.org/10.4095/330903
ISBN 978-0-660-45860-1
Catalogue No. M183-7/5-2022E-PDF

This publication is available for free download through GEOSCAN (https://geoscan.nrcan.gc.ca/).

Recommended citation

Rice, J.M., Paulen, R.C., Ross, M., McClenaghan, M.B., and Campbell, H.E. 2022. Quaternary geology of the south Core Zone area, Quebec and Labrador; Geological Survey of Canada, Preprint 5, 58 p. https://doi.org/10.4095/330903

The final version of this manuscript will be released in the following volume:
McMartin, I. (ed.), in press. Surficial geology of northern Canada: a summary of Geo-mapping for Energy and Minerals program contributions; Geological Survey of Canada, Bulletin 611.

Table of Contents

ABSTRACT

The complex glacial geomorphology of east-central Quebec and western Labrador has resulted in conflicting ice sheet reconstructions leaving many questions regarding the behaviour of large ice sheets within their inner regions. Specifically, the ice-flow chronology and subglacial conditions remain poorly constrained. To address this, surficial geology investigations were conducted across the border of Quebec and Labrador. A complex glacial history consisting of five ice-flow phases influenced by regional ice stream dynamics was identified, including a near-complete ice-flow reversal. During each ice-flow phase, the subglacial thermal conditions fluctuated both spatially and temporally, resulting in palimpsest glacial dispersal patterns. Deglacial ages from samples collected as part of this research confirm deglaciation occurred relatively rapidly around 8 ka. The results of this work improve our understanding of the glacial history of an inner region of the Laurentide Ice Sheet and have important implications for mineral exploration in the southern Core Zone area.

RÉSUMÉ

La géomorphologie glaciaire complexe du centre-est du Québec et de l'ouest du Labrador a donné lieu à des reconstitutions conflictuelles de l'inlandsis, laissant de nombreuses questions sur le comportement des grandes calottes glaciaires dans leurs régions internes. Plus précisément, la chronologie de l'écoulement glaciaire et les conditions sous-glaciaires demeurent mal définies. Pour répondre à ces questions, des études en géologie de surface ont été menées à la frontière du Québec et du Labrador. Une histoire glaciaire complexe composée de cinq phases d'écoulement glaciaire influencées par la dynamique régionale des courants glaciaires a été identifiée, y compris une inversion presque complète de l'écoulement des glaces. Au cours de chaque phase d'écoulement glaciaire, les conditions thermiques sous-glaciaires ont fluctué à la fois dans l'espace et dans le temps, ce qui a entraîné des patrons de dispersion glaciaire palimpsestes. Les âges de la déglaciation provenant des échantillons collectés dans le cadre de cette recherche confirment que le retrait glaciaire s'est produit relativement rapidement vers 8 ka. Les résultats de ces travaux améliorent notre compréhension de l'histoire glaciaire d'une région intérieure de l'Inlandsis laurentidien et ont des implications importantes pour l'exploration minérale dans la région sud de la Core Zone.

Volume editor's timeline:
Received May 18, 2020
Revised March 4, 2021
Accepted March 15, 2021

INTRODUCTION

The geologically complex region straddling the border of east-central Quebec and western Labrador (Fig. 1) has an unresolved ice-flow chronology with contradicting relative ages (e.g. Veillette et al., 1999; Jansson et al., 2002) and few geochronological constraints on the timing of ice-margin retreat (e.g. Carlson et al., 2007; Ullman et al., 2016; Dubé-Loubert et al., 2018; Dalton et al., 2020). Prior to our research, only small-scale (1:1 000 000) surficial maps and sparse field datasets were available. The lack of geoscience data largely stems from the vastness and remoteness of the region, making it difficult to collect field-based data and constrain numerical models of the Laurentide Ice Sheet (LIS). These models predict a low probability of warm-based conditions and limited subglacial erosion within this region (e.g. Tarasov and Peltier, 2004; Stokes et al., 2012; Melanson et al., 2013), but are at odds with empirical evidence of a migrating ice divide and observations of significant glacial dispersal distances, typically associated with warm-based subglacial conditions (e.g. Klassen and Thompson, 1993). Developing a better understanding of the relative chronology and erosional intensity of ice-flow events, and the resulting glacial dispersal patterns, will offer important insights into ice sheet dynamics and provide a beneficial framework for drift prospecting in glaciated terrains. The region is of particular interest as glacial dispersal patterns could help refine bedrock geology in regions where bedrock outcrops are sparse (Fig. 2; Corrigan et al., 2015, 2016, 2018; McClenaghan et al., 2017). This publication provides an extensive review of previous work in the region and presents a new ice-flow chronology and resulting glacial dispersal patterns that were developed through detailed surficial mapping and till provenance studies conducted during the Geo-mapping for Energy and Minerals (GEM2) Hudson-Ungava Core Zone surficial mapping activity.

Previous work

Paleo-ice sheet reconstruction

Ice-flow histories

Geological Survey of Canada (GSC) geologist Albert Peter Low was the first to conduct geological fieldwork in the southern Hudson-Ungava region. Based on the radial pattern of outcrop-scale ice-flow indicators measured during his expedition, he inferred the region was an area of significant ice accumulation, characterized by outward ice flow in all directions (i.e. an ice outflow centre) and also the centre for ice sheet recession (Low, 1896). The central Quebec-Labrador region is now well established as one of the largest regions of ice accumulation and dispersal of the LIS, commonly referred to as the Quebec-Labrador dome (Kleman et al., 2002; Jansson et al., 2003; Occhietti et al., 2004; Stokes et al., 2012), although exact areas of inception and early growth are unknown (e.g. Dyke and Prest, 1987). Historically, this region has also been referred to as the New Quebec dome (Hillaire-Marcel et al., 1981; Vincent, 1989; Roy et al., 2015).

This region is characterized by a U-shaped boundary between streamlined glacial landforms converging toward Ungava Bay and radiating away, defined by a relatively sharp boundary (Fig. 3A). This pattern was interpreted by Douglas and Drummond (1955) and Wilson et al. (1953) as the position of a major ice divide of the Quebec-Labrador sector of the LIS. Hughes (1964), in contrast, interpreted the U-shaped boundary to be the result of ice-flow into Ungava Bay being younger than the radial flow in at least a part of the boundary area, and hence did not necessarily indicate the location of a divide. Despite this, the divide location was continuously used for decades during subsequent ice-flow reconstructions at least along its eastern arm (e.g. Prest, 1970; Fulton and Hodgson, 1979; Dyke et al., 1982).

Detailed field investigations of the region began in the early 1980s when Klassen and Bolduc (1984) reported an old ice-flow event to the northeast, during field work south of the Smallwood Reservoir, near Churchill Falls (Fig. 1). This early work was followed up by a larger field project by Klassen and Thompson (1987, 1988, 1989, 1993) across western Labrador and parts of east-central Quebec. During this research project, over 300 striation measurements, supplemented by glacial erratic tracing and landform analysis, were used to identify five ice-flow phases that occurred over a large region of western Labrador and east-central Quebec (Fig. 3B). The oldest ice-flow phase (Event I) was to the northeast, with striation evidence recorded within the study area and as far as 300 km northeast to the Labrador coast. Klassen and Thompson (1993) used northeast dispersal of different bedrock lithologies to indicate that this ice-flow phase affected all of Labrador, but found little evidence of Event I in western Labrador or east-central Quebec, where associated early phase ice-flow vectors become indistinguishable from later ice-flow trajectories. During Event I, Klassen and Thompson (1993) suggested the ice divide was located to the southwest of Churchill Falls (*see* Fig. 1 for location), somewhere north of the St. Lawrence River, in a position much further south than during later ice-flow phases, which they used as evidence to indicate Event I occurred early within, or prior to, the Wisconsin glaciation. Following Event I, the ice divide migrated north and was oriented northwest/southeast resulting in ice flowing radially to the southwest, east-southeast, and east-northeast (Event II), and was attributed to the Last Glacial Maximum (LGM) (Fig. 3B). The converging oriented glacial landforms toward Ungava Bay (Fig. 3A) were attributed to Event III with northwest ice flows that propagated from an ice divide located somewhere near Schefferville all the way to Ungava Bay. Crosscutting landforms and striations were used as evidence that Event III was followed by a younger radial ice-flow phase (Event IV) that propagated somewhere near the Caniapiscau Reservoir with ice flowing to the southeast south of the Smallwood Reservoir changing to east then northeast flow north of the Smallwood Reservoir (Fig. 3B). These four main regional-scale ice-flow events were followed by a more localized late-glacial event represented by fine, shallow striae indicating a northeast ice flow to the north of the Smallwood Reservoir and eastward ice flows influenced more locally by topography toward the Labrador coast (Fig. 3B). Later work by Liverman and Vatcher (1992, 1993) using surficial mapping and till sampling in the Schefferville region supported the reconstruction of Klassen and Thompson (1993), with only some local variations in late ice-flow phases caused by topographic highs.

In addition to their relative ice-flow chronology, Klassen and Thompson (1993) investigated drift composition and glacial erratic dispersal patterns. Through their work, they concluded that four of the ice-flow events accounted for the bulk of the glacial sediment dispersal: Event I (northeast), Event II (east/southeast/northeast), Event III (northwest), and Event IV (southeast/east/northeast).

While Klassen and Thompson (1993) focused their work largely to the east of the U-shaped boundary, Veillette et al. (1999) investigated the central and southeastern parts of the boundary along the Caniapiscau Reservoir, which allowed inspection of large areas of pristine, freshly exposed bedrock surfaces by boat, thus providing exceptional conditions for a detailed analysis of striated surfaces not found under standard field conditions. This work provided additional evidence, both in the striation and landform records, to support Hughes' (1964) interpretation that the U-shaped boundary was the capture limit of the warm-based Ungava Bay ice-flow events (i.e. that the boundary was an unconformity, not a divide). It also generally supported the ice-flow reconstruction for the area to the east proposed by Klassen and Thompson (1993). Within the Caniapiscau reservoir area, Veillette et al. (1999) also identified a presumed, pre-Wisconsin ice-flow event, citing north-northeast striated surfaces that are stained by a ferromanganese varnish and are truncated by unstained striated surfaces formed by subsequent ice-flow phases. Klassen and Thompson (1993) had also found rare occurrences of an "old" north-northeast ice flow on striated surfaces, which they attributed to an ice mass located somewhere in

the Laurentian Highlands north of the St. Lawrence River. Further evidence of possible pre-Wisconsin ice-flow events includes the suspected pre-Wisconsin till deposits reported in the Wabush area ~ 200 km southwest of the current study (Fig. 1) area by Klassen et al. (1988). Additionally, Granberg and Krishnan (1984) reported peat buried beneath 18 m of glaciofluvial sediments which are overlain by till and found on the lee-side of a steep bedrock scarp near Schefferville. However, wood from the peat layer yielded an age of 24 250 ± 600 yrs BP, indicating the region was ice-free near the end of the Middle Wisconsin. However, no other data on pre-Late Wisconsin sediments have been published for the region and older pre-LGM, conventional radiocarbon dates should be interpreted with caution (e.g. Reyes et al., 2020). The hypothesis of an older (i.e. prior to Marine Isotope Stage (MIS) 5a) glaciation that would have originated from the Laurentian Highlands is speculative and evidence of interglacial deposits remains limited to only a few observations.

Jansson et al. (2002) disagreed with the glacial reconstructions of Hughes (1964), Klassen and Thompson (1993), and Veillette et al. (1999), and instead suggested that the ice centre, at the start of the ice margin retreat, was located just south of Ungava Bay (purple arrows- Fig. 3C). Jansson et al. (2002) used aerial photograph interpretations and fieldwork in the Caniapiscau Reservoir region to support their findings that ice flowed radially from the cold-based ice centre as the ice dome began to shrink. They suggested cold-based glacial conditions preserved landforms (associated with pre-LGM phase; black arrows in Fig. 3C) in the interior of the Quebec-Labrador region (shaded region of Fig. 3 inset). Follow-up work by Clarhäll and Jansson (2003) near Lac aux Goélands supported a change in subglacial dynamics that resulted in the preservation of older landforms (pre-LGM flow-Fig. 3D and Fan B-Fig. 3C) under cold-based conditions during later ice-flow phases (LGM Flow-Fig. 3D and Fan C-Fig. 3C), conflicting with the ice-flow reconstruction of Klassen and Thompson (1993) and Veillette et al. (1999; Fig. 3B).

More recently, just north of the current study area, Dubé-Loubert (2019) reported detailed striation and landform evidence for an old ice-flow phase to the northeast, similar in orientation to Event I of Klassen and Thompson (1993) and the oldest flow of Veillette et al. (1999). Additionally, Dubé-Loubert (2019) indicated that an ice divide formed along the George River valley and separated flow to the west-northwest on the west side of the river from ice flow to the east-northeast on the east side. This divide was inferred to have been active during LGM, as previously suggested by Dyke and Prest (1987). Dubé-Loubert (2019) interpreted at least the eastern arm of the U-shaped boundary as an ice divide position. How far south this divide extended is currently undefined. Dubé-Loubert (2019) also indicated that the landscape to the west of the divide consisted of a mosaic of landform assemblages from different ice-flow phases, with the youngest phase related to highly dynamic ice streams flows north-northwest toward Ungava Bay. East of the divide, older ice-flow phases are crosscut by ice streaming associated with the Kogaluk (Strange Lake) Ice Stream (Margold et al., 2015). These results coupled with ^{10}Be and ^{26}Al abundances indicated that only small patchy regions were sustained cold-based throughout the last glaciation (Dubé-Loubert, 2019).

Ice margin retreat

Early work confining the pattern and timing of ice margin retreat in the Quebec/Labrador region focused on ^{14}C dating of material from raised beaches and reconstruction of isostatically tilted strandlines (Ives, 1958, 1960a, b; Matthews, 1961). From this work, it was suggested that the ice sheet fragmented into small ice caps during deglaciation. Subsequent work by Lauriol and Gray (1987) analyzing the distribution and orientation of eskers across the region supported the separation of the ice sheet into smaller ice masses during deglaciation. Clark et al. (2000) also supported ice-sheet fragmentation into smaller ice caps. These small ice caps would have been required to block meltwater

drainage and allow for the formation of the proglacial lakes identified across Quebec and Labrador. Additionally, they suggested the retreat pattern was highly asymmetrical, with rapid southern retreat toward a cold-based ice centre, causing the centre to migrate ~ 500 km to the north from its earlier LGM position (around 51°N) while continuously maintaining cold-based conditions during retreat. This northward migration was suggested to be the result of a thinning cold-based ice mass that eventually fragmented and disappeared about 5 ^{14}C ka BP, preserving the existing glacial landforms under cold-based conditions. Later work by Ullman et al. (2016) suggested a similar rapid ice margin retreat as indicated from ^{10}Be deglacial ages from large erratic boulders along a ~ 400 km transect (Fig. 4).

Glacial lake reconstructions and constraints on deglaciation

During ice margin retreat of the Quebec-Labrador sector, many glacial lakes formed at the margins of the retreating ice mass (e.g. Clark et al. 2000; Dyke, 2004). Within our study area drainage to the north was blocked in the George River and Rivière à la Baleine valleys (GR and RdB respectively on Fig. 4) creating glacial lakes Naskaupi and McLean, respectively (Ives 1960a, b; Barnett, 1967; Barnett and Peterson, 1964; Clark and Fitzhugh, 1990; Dubé-Loubert et al., 2018). Lake Naskaupi was first identified from its raised shorelines by an early 20th century explorer (Prichart, 1911) and was formally named Lake Naskaupi by Ives (1958, 1960a). Five lake levels (N1-N5) were described in detail (Henderson, 1959; Mathews, 1961; Barnett and Peterson, 1964). In the Lac aux Goélands area, Peterson (1965; their Fig. IIIb) mapped the N2 levels as far south as 55°30' N. As the drainage divide is just south of this area, this extent required ice dams to the south and west to prevent drainage. Recent investigations have confirmed the first four lake levels for Lake Naskaupi (N1-N4), with minor, transient stages between them (Dubé-Loubert and Roy, 2017). The main lake level (N2') is interpreted to have occupied two basins that were separated by a block of cold-based ice (Dubé-Loubert and Roy, 2017). The southern basin, which extended into the northeast part of our study area, had an average depth of 50 m and formed distinct shorelines.

In the northwestern, another glacial lake inundated the study area and was named McLean by Wallace (1932) after the Hudson Bay Company employee John McLean, who first recognized the shorelines. The timing of lake inundation is unknown but was likely around the same time as the maximum extent of Lake Naskaupi (N2'). During N2' (472 m), Lake McLean, in the Rivière à la Baleine valley (Fig. 4), was periodically connected to lake Naskaupi via several overflow channels with overflow going into lake Naskaupi north of the study area (Dubé-Loubert and Roy, 2017). Five levels were initially mapped for Lake McLean (Mc1 to Mc5) with its main stage (Mc2) evolving independently of Lake Naskaupi (Ives, 1960b). The shorelines of Lake McLean record smaller lake level variations than Lake Naskaupi (~30 m variation for McLean and ~ 60 m for Naskaupi). Lake McLean was also not as extensive or deep as Lake Naskaupi and, as a result, has less well-developed shorelines (Barnett, 1967).

In the southern part of the study area, Low (1896) described terraces along the shores of Lake Michikamau (western half of the Smallwood Reservoir), boulder-strewn raised shorelines and flat-topped islands, all influenced by an unnamed post-glacial ice-dammed lake occupying this region. Follow-up work by Tanner (1948) suggested that an ice dam was needed to the south of (then) Lake Michikamau for this lake to develop. Ives (1960b) and Peterson (1965) both recognized these shorelines south of the drainage divide, near the eastern arm of the Smallwood Reservoir and, given the limited data available, concluded they were most likely ice-pushed ramparts. This region was subsequently flooded to create the Smallwood Reservoir with the construction of the Churchill Falls hydroelectric dam in 1974, resulting in the submergence of many of these shorelines.

These glacial lakes are critically important in constraining ice margin retreat and provide important controls on the overall deglacial patterns of the Quebec-Labrador sector of the LIS. This is exemplified by Clark et al. (2000), who used glacial lakes McLean and Naskaupi, along with other ice-marginal lakes, to constrain ice margin retreat patterns, although the timing of many of these lakes remains poorly defined. The lack of organic-rich lake sediments commonly used for ^{14}C dating within the interior of the Quebec-Labrador region and the shortage of well-developed glaciolacustrine shorelines suitable for optical dating have made constraining the ages of these glacial lakes difficult.

More recently, cosmogenic ^{10}Be exposure dating has improved our understanding of the timing and pattern of ice margin retreat for the Quebec-Labrador sector (Fig. 4; Clark et al., 2003; Carlson et al., 2008; Ullman et al., 2015, 2016- Fig. 4). Collectively, these investigations indicate the region west of the Caniapiscau Reservoir was ice-free by 8.2 ± 0.5 ka and the region south of the Churchill River was ice-free no later than 6.7 ± 0.4 ka, indicating a rapid retreat of the ice margin. North of the study area, ^{10}Be exposure ages of imbricated boulders deposited along raised shorelines and related to the catastrophic drainage of Lake Naskaupi during N2' indicate that the lake at least partially drained around 8.3 ± 0.3 ka (Dubé-Loubert et al., 2018). Dyke (2004) encompassed the entire Naskaupi and McLean lake sequences to have occurred between 8.5 and 7.5 ka. However, there are no age constraints for shorelines at the southern extent of Lake Naskaupi (although assumed to have occurred during N2') and no age constraints are available for Lake McLean or glacial lakes in the Smallwood Reservoir area.

Surficial mapping

Douglas and Drummond (1955) created the first small-scale glacial landform map of the Labrador Peninsula through aerial photograph interpretation and field observations. Later work resulted in surficial geology maps published at 1:1 000 000 and 1:5 000 000 scales for the study area (Klassen et al., 1992; Fulton, 1995). More local-scale surficial maps were completed for the surrounding area, with some preliminary surficial maps of the Labrador portion of the study area (Klassen and Paradis, 1990). Ives (1956) brought attention to 'rippled till' west of the study area and discussed the geomorphological relationship of the till with the numerous eskers in the area, proposing a possible link between the two landform systems. However, follow-up work by Cowan (1967) indicated no relationship between the ribbed moraine (rippled till) and eskers or esker fans, based on field investigations carried out 60 km south of Schefferville. Cowan (1967) concluded that the ribbed till was formed by overriding ice bulldozing material until it accumulated and provided enough resistance to the ice, that the ice then overrode the material and continued to advance, repeating the process. Jansson et al. (2003) and Jansson (2005) mapped a small part of the study area, as well as a region to the west and northwest of the study area in more detail, and indicated that the region had a much more complex glacial history than previously reported. The surrounding surficial maps did identify important landforms and striation trends for use in ice-flow reconstructions but did not cover the entire study area and lacked detailed separation of surficial units required for modern ice sheet modelling studies (e.g. Gowan et al., 2019).

Till geochemical and indicator mineral dispersal patterns

Klassen and Thompson (1993) conducted an extensive till geochemical survey in western Labrador and parts of east-central Quebec, including the current study area. They identified multiple glacial dispersal patterns formed by early ice-flow phases and modified during later ice-flow phases creating different footprints based on their geographical location. Along the Quebec-Labrador border, near what would have been the interior of the Quebec-Labrador sector the dispersal of iron formation clasts during multiple ice-flow phases in various directions from their source created an ameboid dispersal pattern (grey scale in Fig. 5). However, toward the coast, dispersal patterns become more linear (e.g. Red Wine Complex (yellow fan) and Flower River suite (green fan; Fig. 5)) as the result of a single

or several ice-flow phases in a relatively uniform regional direction. Although Klassen and Thompson (1993)'s dispersal patterns reflect their regional ice-flow phases, their sample survey was limited in extent (i.e. did not cover the full extent of the iron formation dispersal) and in analytical techniques (i.e. did not use modern total digestion geochemical analysis). Additionally, the dispersal of iron formation clasts was based on a qualitative assessment of whether erratics were absent, rare, present, common, or abundant. Follow-up work by Klassen and Knight (1995) used Inductively Coupled Plasma-Atomic Emission Spectrometry (ICP-AES) and Instrumental Neutron Activation Analysis (INAA) to reanalyze over 2000 till samples collected across Quebec and Labrador. Through this follow-up work, glacial dispersal patterns were identified from till matrix geochemistry, similar to those determined from erratic boulders, albeit with much shorter dispersal distances (e.g. Klassen and Knight, 1995- Figure 11, pg. 34- Pb sourced from the Labrador Trough).

More recently, Brushett and Amor (2013) identified distribution patterns of elevated chromite grain abundances (3-6 grains) in regional esker samples in the southwest part of the study area, which indicated east-southeast transport from a source located somewhere within the Labrador Trough, and elevated abundances of pyrite grains (6-50 grains). Additionally, a few gold grains were identified in samples collected from eskers that extend southeast across the study area. These indicator minerals are thought to have originated from a source within the Labrador Trough, or, within the Ashuanipi complex just west of the Labrador Trough. These prior works on till geochemistry and indicator minerals suggest that glacial dispersal patterns are more complex toward the interior of the Quebec-Labrador sector than in the outer regions toward the Labrador Coast.

Study area

Location and Physiography

The study area straddles the provincial border between Quebec and Newfoundland and Labrador ~ 60 km east of Schefferville, Quebec and covers over 30,000 km^2 within the Wood Lake (NTS 23-I) and Lac Résolution (NTS 23-P) map sheets, between 64° and 66°W longitude and 54° and 56°N latitude (Fig. 1). The largest lakes are the Smallwood Reservoir in the south, Lac Champdoré in the northwest, Lac aux Goélands in the east, and Lac Mistinibi in the northeast. The northern half of the study area is characterized by discontinuous permafrost (50-90%), often expressed by the presence of frost boils (Smith, 2010). In the southern half, conditions transition to sporadic, discontinuous permafrost (10-50%). The study area straddles the drainage divide between rivers flowing north/northwest to Ungava Bay and rivers flowing east/southeast to the Atlantic Ocean. The George River drains northward from the divide to where it joins the De Pas River and flows through a large river valley (George River valley) into Ungava Bay (Fig. 4). The topography within the study area is typical of Canadian Shield terrain, with undulating low to moderate relief and irregular bedrock knobs. Elevations range from less than 350 m in the George River valley to 704 m on the highest rock knob near the continental drainage divide. Hills and upland regions typically have outcrops with veneers of glacial sediments and are flanked by thicker glacial deposits in the valleys.

The study area is within the physiographic regions of the Lake Plateau within the James Region and the George Plateau and Whale lowland divisions of the Davis region, all of which are within the Canadian Shield physiographic region (Bostock, 2014). Ecologically, the region transitions from Taiga Shield zone in the north into Boreal Shield zone in the south (Smith, 2010). The tree line crosses the northern part of the study area with trees typically growing only in the low-lying areas. Moss, lichen, and small shrubs dominate the highland areas, with black spruce and tamarack (larch) comprising much of the lowland forests.

Bedrock geology

The study area is located within the southern Core Zone, a Precambrian lithotectonic terrane of the eastern Canadian Shield (Wardle et al., 2002). The Core Zone is within the Southeast Churchill Province and extends ~ 500 km from the Grenville Orogen in the south to Ungava Bay in the north (Fig. 2). It is bounded to the west by the New Quebec Orogen and the east by the Torngat Orogen. Two major shear zones transect the region, the Lac Tudor shear zone and the Rivière George shear zone (Fig. 2). These shear zones mark the eastern and western boundaries of the George River Domain, which consists of the De Pas Batholith, a large felsic intrusion that forms a prominent upland and its associated orthogneisses which bisects the study area (Corrigan et al., 2018). The batholith is a K-feldspar porphyritic monzogranite-granodiorite-syenogranite, with more orthopyroxene-rich assemblages in the western half and more hornblende-biotite-rich rocks in the east (Sanborn-Barrie, 2016).

East of the George River Domain, in the northern half of the study area, is the Mistinibi-Raude Domain (Fig. 2), a complex of supracrustal rocks and plutonic rocks of Neoarchean and Paleoproterozoic age (van der Leeden et al., 1990). The Mistinibi-Raude Domain is capped by the Lac Zeni amphibolite, and mylonitic tonalities in the south, which are both bounded to the east by Mesoproterozoic granites. In the southeast part of the study area, the Core Zone is intruded by Mesoproterozoic plutons and is bounded to the south by the Seal Lake Group (Sanborn-Barrie, 2016) and the Michimikau granite and anorthosite suite of rocks (Fig. 2). In the northwest part of the study area, the Tudor Lake shear zone marks the boundary between the George River Domain and the Rachel-Laporte metasedimentary rocks to the west. The Rachel-Laporte rocks overlie Churchill Province basement rocks in the north of the study area (Fig. 2). South of the Rachel-Laporte Domain, Churchill Province basement rocks are overlain by metavolcanic rocks of the Labrador Trough. The Paleoproterozoic Labrador Trough includes the Kanipiskau Supergroup which is composed of the Knob Lake Group that hosts economic iron deposits in the west and the Doublet Group in the east (Wardle, 1982; Corrigan et al., 2015). For a detailed summary of the lithological assemblages within and surrounding the study area see James et al. (1993, 1996), Clark and Wares (2005), Sanborn-Barrie (2016), and Corrigan et al. (2015, 2018).

Surficial geology

Surficial mapping as part of the GEM2 activity shows the northern part of the study area is characterized by highland clearings covered in till veneer with abundant small bedrock outcrops and erratics (Rice et al., 2017c, 2017d; Paulen et al., 2020c, 2020d). These uplands are flanked by thicker till blankets in the valleys. Evidence of meltwater reworking and meltwater erosion is also abundant in the north, which includes glaciofluvial deposits, a few eskers, kames, and lateral meltwater channels. In the southern half of the study area, organic deposits are much more abundant in the low-lying areas and the esker network is denser and more continuous, with only rare meltwater channels (Paulen et al., 2017, 2019a, 2019b). Wave-washed bedrock, winnowed till deposits and beach sediments occur in areas inundated by glacial lakes Naskaupi, McLean and Low (see Deglacial chronology section below).

METHODS

Ice-flow measurements

As part of surficial mapping activities, ice-flow directions were determined by measuring streamlined glacial landforms (e.g. crag-and-tails, drumlins, and large-scale glacial lineations) from both satellite imagery and aerial photograph interpretation. Landsat 8 satellite image mosaics were coupled

with the highest resolution data available, a hillshaded digital elevation model (DEM from 30 m resolution Shuttle Radar Topography Mission (SRTM) data), following procedures outlined by Clark et al. (2000) and Stokes and Clark (2001). The DEM was coupled with regional bedrock and aeromagnetic maps to ensure the mapped landforms were not bedrock features. During field work conducted between 2014 and 2016, outcrop-scale ice-flow indicators (e.g. striations, grooves, rat tails, and mini-crag-and-tails; Fig. 6) were measured to further clarify the direction of ice-flow. The directions of striations and grooves were determined from the shape of the outcrops, including plucking directions. Where multiple sets of ice-flow indicators were identified, relative ages were determined through the examination of older ice-flow indicators in protected lee-side positions on bedrock outcrops (e.g. Veillette and Roy, 1995; McMartin and Paulen, 2009). Once a relative ice-flow chronology was established from outcrop-scale indicators, it was compared to the surrounding landform record to derive more regional-scale flowsets and chronology. Because glaciated terrains are typically fragmented within inner regions of ice sheets (e.g. Gauthier et al., 2019), ice-flow indicator patterns (both landform flowsets and outcrop-scale records) were analyzed across the study area to determine whether disjointed zones with internally coherent records could be identified. This is an important step in the identification and characterization of different palimpsest glacial footprints (e.g. Kleman and Glasser, 2007). In this conceptual model, unmodified older ice-flow indicators are preserved due to a shift from warm-based active ice to cold-based, non-erosive ice. Typically, these relict, unmodified terrains are identified next to an area where they are variably overprinted by later ice-flow phases. Therefore, when conducting ice-flow measurements, several inherent assumptions were made including the assumption that subparallel ice-flow indicators on any given polished surface were formed contemporaneously during a single ice-flow phase.

Till sample collection and analysis

Till samples were collected across the study area for indicator mineral studies, till matrix geochemistry analysis, and pebble lithology counts. Till was sampled at a spacing of approximately 8-12 km, using protocols established by the Geological Survey of Canada (McClenaghan et al., 2013, 2020; Plouffe et al., 2013). The sediment targeted for sampling was determined to be subglacial till based on its poorly sorted nature, the abundance of striated and faceted clasts within the sediment, and a high degree of compaction. Till samples were collected from hand-dug pits in frost boils or in soil profiles where the C-horizon (unoxidized) till was targeted. During sample collection, larger pebbles (>64 mm) were removed by hand to minimize the sample weight. At each sample location (n=306 sites), a ~ 3 kg sample was collected for till-matrix geochemistry analysis. At 259 of those locations, an additional ~ 10 to 15 kg sample was collected for indicator mineral recovery and clast (>2 mm) separation. Field data for collected samples are summarized in Rice et al. (2020a).

For this study, 306 samples collected in 2014, 2015, and 2016 were submitted for till matrix geochemical analysis in addition to 30 archived GSC samples collected in 1986 and 1987 by Klassen and Thompson (1993). Additionally, 257 samples were submitted for indicator mineral analysis and 256 samples underwent clast lithology classification. Detailed descriptions of the geochemical methodologies, including quality assurance and quality control methods, are reported in McClenaghan et al. (2016a) and Rice et al. (2017a). Similarly, sample preparation and analysis for indicator minerals are reported in McClenaghan et al. (2016b, 2017) and Rice et al. (2017b). Detailed methodology for clast lithology classification is reported in Rice et al. (2017b, 2020b). For this publication, selected indicator mineral and geochemical results are presented to support our ice-flow reconstruction. For the full results of these analyses and a complete list of all published reports from this research program, including published surficial maps, refer to Appendix A.

Geochronological sampling

To constrain the timing of deglaciation within the study area and better understand the paleoglaciological evolution of the Quebec-Labrador sector during ice sheet collapse, geochronological samples were collected. Two types of geochronological assessments were utilized in this investigation: optically stimulated luminescence (OSL) dating and cosmogenic ^{10}Be surface exposure age determination. The use of OSL dating to approximate the timing of glacial lake beach formation has been conducted successfully in other glaciated regions (e.g. Lepper et al., 2013; Hickin et al., 2015). Using similar methods, samples were collected from coarse-to-fine-grained sands from the beach ridges of the glacial lakes identified within the study area. For this study, OSL analysis was conducted on feldspar grains as the quartz grains lacked the "fast acting component" required for accurate analysis (see Rice et al., 2019 for details on methods).

Samples of glacially eroded bedrock and glacial erratics were also collected for ^{10}Be exposure dating. At nine sites, a single bedrock sample was collected from elevated, windswept outcrops from lithologies with high (>35%) quartz content. At two of the bedrock sample sites, erratic boulders were also collected (15-PTA-081E and 15-PTA-077E). Boulders were selected for sampling based on their quartz content (quartz > 35%), size (> 1 m^3), stability (no evidence of post-depositional movement), and absence of topographic shielding. Ages were calculated using the online exposure age calculator v.3 (http://hess.ess.Washington.edu) using the Baffin Bay/Arctic ^{10}Be production rate (Young et al., 2013) and the nuclide- and time-dependent scaling scheme (LSDn; Lifton et al., 2014). All ^{10}Be results reported in this study are treated as 'apparent ages' due to the potentially added uncertainty caused by cosmogenic nuclide inheritance (e.g. Rice et al., 2019). In an attempt to determine the rate of ice margin retreat, ^{10}Be samples were collected along an east to west transect parallel to previously inferred ice margin retreat direction (Dyke, 2004). An additional bedrock sample was also collected in the southern half of the area (15-PTA-114) to assess if deglacial ages were similar to those in the north. All ages reported for ^{10}Be exposure dating and OSL are reported as years before measurement in thousands of years (ka). The ^{10}Be ages are reported with 1σ analytical error and OSL ages are reported to 2σ analytical error as is standard for each analytical process (Aitken, 1998; Dunai, 2010).

RESULTS AND INTERPRETATIONS

Relative ice-flow chronology

Streamlined landform mapping identified 1455 crag-and-tails and 1322 drumlinoid ridges across the study area (Fig. 7). Additionally, 403 outcrop-scale ice-flow indicators were measured at 247 locations across the study area. Through the mapping of landforms and measurement of striations, regional flowsets were identified and their relative age established and then grouped into five ice-flow phases, which are summarized below.

Flow 1

The earliest ice-flow phase identified was to the northeast. This phase is most evident in flowsets in the northeast of the study area (Figs. 7 and 8) but is also correlated to the oldest striations observed elsewhere in the study area (Fig. 8). Flow 1 was remarkably uniform in direction with only slight deviations in measured striae azimuths (Fig. 8). The lack of striation evidence of this ice-flow phase in the west-central part of the study area is likely due to subsequent erosion of bedrock by later ice-flow phases. The wide distribution of these relatively uniform ice-flow indicators suggests that this phase was warm-based and erosive over much of the study area. Flow 1 was the oldest ice flow at every location

except for three sites (15-PTA-147 (345°), 16-PTA-171 (311°), and 16-PTA-154 (350°)), where an even older flow to the north-northeast was noted.

Our Flow 1 is equivalent to Event I of Klassen and Thompson (1993). This ice-flow phase has been identified as one of the oldest phases in the striation record across central Quebec and western Labrador and has been hypothesized to have originated somewhere in the Laurentian Highlands (Klassen and Thompson, 1993; Veillette et al., 1999; Parent et al., 2004). The absolute age and duration of this phase are unknown, but it has been attributed to the LGM and early deglaciation of the larger Quebec-Labrador sector, when the ice margins were offshore (Dyke and Prest, 1987). No evidence of non-glacial inter-till units was observed in our study area, nor was evidence of ferromanganese staining on any observed outcrops. In contrast to Veillette et al. (1999) who worked within the lowlands of the Caniapiscau Reservoir, our striation observations were made largely on upland areas limited to access by helicopter.

Flow 2

The ice-flow direction and subglacial conditions changed drastically after Flow 1 as indicated by the degree of preservation of Flow 1 features in the northeast part of the study area and by strong overprinting in the northwest by north-northwest Flow 2 indicators (Figs. 7 and 9). This suggests that conditions changed from broad warm-based conditions to more regionally cold-based conditions except for restricted regions of actively sliding ice mainly in the northwest (e.g. Rice et al., 2020d). Flow 2 overprints Flow 1 indicators at six locations and is overprinted by later ice-flow indicators (Flow 3) at eight locations, which was used to determine its relative chronology. Flow 2 striations are oriented more toward the west in the central part of the study area where landforms are noticeably absent (Fig. 7). In the central highlands, where evidence of Flow 2 only remains on striated bedrock surfaces, there was either not enough sediment to produce landforms or subglacial conditions were not conducive to producing landforms (i.e. the highlands were too close to the divide to form landforms). The hypothesis that an ice divide occupied the northeastern part of the study area is supported by the preservation of landforms associated with Flow 1 east and southeast of the Flow 2 "footprint" and by old southeast-trending landforms occurring in the southeast of the study area (Fig. 7). Although no striation evidence of Flow 2 was identified in the southeast, the southeast-trending landforms are overprinted by more easterly Flow 3 landforms and consequently must have formed prior to Flow 3 (Fig. 10). Therefore, we suggest that ice flowed in nearly opposite directions from an ice divide located across the study area (Fig. 9) or as the ice divide migrated east to west.

Flow 2 is similar in orientation to Event III of Klassen and Thompson (1993) and the northwest ice-flow phase of Veillette et al. (1999) but our relative chronology differs from these authors in that our Flow 2 occurred before a major eastward phase (their Flow II and IIb). Flow 2 is also similar in orientation to Flowset 19 of Clark et al. (2000) and Fan D of Jansson et al. (2003), which were suggested to have formed by ice streaming toward Ungava Bay early on during deglaciation. Jansson et al. (2003) indicated the catchment area of the Ungava Bay ice stream migrated west from its original position on the eastern edge of Ungava Bay. This westward migration could have led to the progressive westward shift of the ice divide across our study area. Alternatively, the ice divide may have shifted as eastward streaming ice propagated up-flow, forcing the divide west. Overall, this ice divide migration led to a near complete ice-flow reversal within a portion of the study area, resulting in the third ice-flow phase (Flow 3).

Flow 3

Irrespective of what caused the westward migration of the divide, ice began to flow eastward toward the Labrador coast during Flow 3 (Fig. 11). Flow 3 outcrop-scale indicators crosscut Flow 2 at eight key locations where they are preserved on the lee sides of Flow 3 sculpted bedrock outcrops. At 15 locations Flow 3 ice-flow indicators were protected (or preserved) from (during) later ice-flow phases. Flow 3 striations are found almost entirely across the study area and are generally oriented to the east. In the northeast, these striations are oriented more to the east-northeast, whereas in the south they are oriented slightly more to the east-southeast. A high density of converging streamlined landforms associated with Flow 3 form an ice stream corridor (Cabot Lake Ice Stream: CLIS; Paulen et al., 2019a; Rice et al., 2020d) in the east-central part of the study area (blue dashed outline-Fig. 7).

Flow 3 is similar in orientation to Events II and IIb of Klassen and Thompson (1993) and to a degree Event V east of the study area (Fig. 3B), and to Jansson et al. (2002) and Clarhäll and Jansson (2003)'s pre-LGM flow (Figs. 3C and 3D), but does not align with either ice-flow chronology. Some of the shorter northeast oriented landforms in the northeast corner of the study area may also be associated with Flow 3, as part of the onset zone of the Kogaluk Ice Stream just northeast of the study area (#187 of Margold et al., 2015). These shorter landforms are slightly askew from the larger northeast landforms oriented to the northeast that formed during Flow 1 (Rice et al., 2020c-their Fig. 3). About 250 km to the southeast of the study area the south-trending Happy Valley-Goose Bay Ice Stream (#186 of Margold et al., 2015) was suggested to have been active at ~ 8.9 ^{14}C ka (Margold et al., 2018). The similar eastward orientation of the Cabot Lake and Kogaluk ice streams and several other ice streams along the Labrador coast suggests that they were operating around the same time, their location controlled, in part, by the numerous fjords along the Labrador coastline.

Flow 4

Evidence of Flow 4 is mainly confined to the southern half of the study area and records a more dynamic south to southeast ice-flow pattern (Fig. 12). Flow 4 overprints Flow 3 at 15 locations and is overprinted by Flow 5 at 25 locations, which was used to determine its relative chronological age. Landforms associated with Flow 4 are abundant in the central part of the study area and are confined to the west side of the central upland (Fig. 7). The orientation of glacial landforms and striations suggests that the eastward ice-flow phase (Flow 3), in the east-central region of the study area, gradually shifted to the south (Flow 4) into a topographically confined lowland corridor west of the central uplands as the ice sheet thinned during deglaciation. Ice flow was then essentially pirated from the central uplands and diverted south, funneled into the Smallwood Reservoir where it began to flow to the east/southeast (Fig. 13; Paulen et al., 2015, 2017). This type of ice-stream piracy has been identified in the Canadian Prairies (Ross et al., 2009), Prince of Wales Island (Dyke et al., 1993), and on eastern Baffin Island (Brouard and Lajeunesse, 2019). Eskers mapped in the southern half of the study are also generally oriented in the same direction as Flow 4 (Fig. 7). The parallel orientation of the eskers to Flow 4 ice-flow indicators suggests they formed shortly after Flow 4 before final deglaciation of the area, when the ice margin had begun retreating, likely to the northwest (Dyke, 2004; Margold et al., 2018). These findings are consistent with regional interpretations that postulate that the shutdown of eastward ice flows to the Labrador coast (Flows 3 and 4) was followed by the formation of subglacial meltwater channels and eskers in the region (e.g. Occhietti et al., 2004).

Flow 4 has a similar orientation to Event IIb of Klassen and Thompson (1993) west of the upland, and to Event II east of the Smallwood Reservoir (Fig. 3B) and was not identified by Jansson et al. (2002) or Clarhäll and Jansson (2003). It should be noted that this Flow 4 is not the same as Flow 4 previously identified by Rice et al. (2019), which correlates with this study's Flow 5 (see below).

Flow 5

The youngest ice-flow phase identified within the study area is Flow 5 (Fig. 14) and represents late-deglacial flows when the ice sheet likely thinned and separated into multiple zones of independent ice flows (Ives, 1958; Kirby, 1962; Clark et al., 2000; Rice et al., 2019). With a lowered glacial profile, the formation of ice-flow indicators was largely topographically controlled (i.e. ice predominantly flowing from local highlands to lowlands). Striations formed by this ice-flow phase have a wide range of orientations but do show a preferential orientation to the northeast. Evidence of this ice-flow phase is often identified as a light glacial polish or short shallow striations on the tops of outcrops, cross-cutting older ice-flow indicators (e.g. Fig. 6). Klassen and Thompson (1993) and Liverman and Vatcher (1992, 1993) also identified topographically controlled late ice flows by a light polish on bedrock outcrops. However, in a small region near Lac Resolution (Fig. 7), streamlined landform from Flow 3 have been reworked by Flow 5, forming smaller landforms oriented to the northeast (purple landforms-Fig. 14 inset). These landforms must have occurred following Flow 3. They are not of the same age as the Flow 1 landforms (black lineations), which are larger and have been reworked by Flow 3 (red lineations) at several sites (Fig. 14 inset). These relative chronology of the landforms correlates well with the striation record observed in nearby uplands.

Deglacial chronology

^{10}Be ages

Ages determined from the most eastern samples (n=4) range between 6.2 ± 2.1 and 9.8 ± 0.2 ka (Table 1; Fig. 15). Samples collected in the centre of the transect (n=3) have the largest range in ages, from 7.1 ± 2.9 to 24.0 ±0.5 ka (Table 1; Fig. 15). Samples collected in the west (n=4) range in age from 7.9 ± 1.8 to 9.5 ± 0.2 ka (Table 1; Fig. 15). The single sample collected for ^{10}Be age determination in the south (16-PTA-114B) has an age of 14.8 ± 0.6 ka, which, along with two samples from the north-central area (16-PTA-070: 24.0 ± 0.5 ka; 15-PTA-077E: 16.7 ± 3.8 ka), are considered to be outliers because they are much older than other samples in the study area and much older than other regional ^{10}Be deglacial ages (Fig. 4; Carlson et al., 2007, 2008; Ullman et al., 2016; Dubé-Loubert et al., 2018). These outliers likely reflect lower glacial erosion. Typically, at least 2-3 m of bedrock material needs to be eroded to completely remove pre-glacial ^{10}Be buildup (Staiger et al., 2006), otherwise, ^{10}Be abundances produce anomalously old ages due to inheritance (see Rice et al., 2019 for details).

OSL ages

An OSL sand sample collected from a beach ridge formed by Lake McLean, above the shores of modern-day Lac Champdoré, yielded an age of 35.0 ± 4.0 ka (Table 2; Fig. 15). This anomalously old age likely indicates that the feldspar grains were not completely zeroed during deposition (e.g. Fuchs and Owen, 2008). Two OSL samples were also collected from raised shorelines of Lake Naskaupi and another from an outwash terrace associated with a lower phase of Lake Naskaupi. The outwash terrace sample (15-PTA-074; elev. 314 m) represents the lowest and latest stage of Lake Naskaupi where beaches were not observed and meltwater channels from stagnating ice masses were feeding into the De Pas River valley. Sample 15-PTA-074 was collected from well-sorted sand with lower flow regime sedimentary structures and yielded a fading corrected age of 7.65 ± 0.99 ka (Table 2). The OSL sample collected from beach sediments at the western edge of Lake Naskaupi (15-PTA-035; 464 m) produced an anomalously old age (61.9 ± 5.02 ka; Table 2). The age from the highest Lake Naskaupi beach (15-PTA-149; 486 m) yielded a fading corrected age of 7.93 ± 0.72 ka (Table 2) and is thought to be close to the true age of the deposit (Rice et al., 2019).

The two OSL samples from a raised beach formed by a lake in the southeast of the study area (465 m) yielded contrasting optical ages (Table 2). Sample 14-PTA-R036 yielded an anomalously old age of 129.5 ± 21.2 ka, which suggests insufficient bleaching of the grains prior to deposition (e.g. Rice et al., 2019). However, results from a second sample collected from the same section (14-PTA-R035) yielded an age of 9.8 ± 0.6 ka (Paulen et al., 2020a). This OSL age could possibly be as young as 8.6 ka with the analytical uncertainty taken into account at two standard deviations. If this age is valid, it would require that either the lake basin was ice-free about 1 to 2 ka earlier than what was suggested by previous ice margin retreat reconstructions (Dyke, 2004; Ullman et al., 2016; Dalton et al., 2020) or this sample was only partially bleached. Given the ages of other beach samples within the study area and regional samples outside the study area (e.g. Dubé-Loubert et al., 2018), an age overestimation is likely.

Till matrix geochemistry

Bedrock lithologies with a distinct geochemical composition that can be recognized in till are limited to the western half of the study area (e.g. metavolcanics, iron formations). A distinct Cu dispersal pattern can be observed around the metavolcanic rocks of the Doublet Zone, with the highest values located within the Zone, decreasing to the northeast, east, and southeast (Fig. 16). Elevated Sb concentrations in the southwestern part of the study area (Fig. 17) reflect the underlying iron formation and associated sedimentary rocks of the Labrador Trough. These are also correlated with elevated Sb concentrations in lake sediments along the entire 800 km length of the Labrador Trough (Amor et al., 2019). Decreasing Sb concentrations are also observed in the northeast, east, and southeast. Base metal values in till samples reflect the composition of local and proximal (up-ice) mineralized rocks in the Labrador Trough and glacial transport to the northeast, east, and southeast.

Indicator minerals

Goethite, a mineral known to be abundant throughout the Labrador Trough's iron bearing formations (Neal, 2000), is observed in highest abundances in the eastern part of the study area with dispersal to the northeast and east (Fig. 18). Within the centre of the study area, orthopyroxene, which was reported to have elevated concentrations in the western orthogneiss (Sanborn-Barrie, 2016), shows a strong eastward dispersal from the source area (i.e. northeast fanning down to southeast dispersal), and a northwestern dispersal pattern in the northwest part of the study area (Fig. 19).

Clast lithologies

Glacial dispersal patterns identified from bedrock lithologies include the dispersal of iron formation clasts to the northeast and east from the Labrador Trough bedrock domain (Fig. 20) and the dispersal of felsic intrusive clasts, predominantly sourced from the George River block, to the east, and to the northwest in the Lac Champdoré area (Fig. 21). It is difficult to determine if the dispersed iron formation clasts are the result of northeast or east transport, or both, partially due to the orientation of the source area that continues to the northwest, outside the study area (Fig. 2). The high concentrations of felsic intrusive clasts in the Lac Champdoré area are probably related to a northwest transport, although quartzofeldspathic units in this area are visually identical to those in the De Pas batholith (Corrigan et al., 2018).

DISCUSSION

Ice-flow chronology and glacial dispersal patterns

The glacial history of the study area is characterized by multiple ice-flow phases, major changes in ice-flow directions and complex glacial dispersal patterns resulting from ice divide migration

(Klassen and Thompson, 1993; Veillette et al., 1999) and related changes in subglacial thermal conditions (Jansson et al., 2002; Clarhäll and Jansson, 2003). Our detailed characterization of these ice-flow phases within the inner regions of the Quebec-Labrador sector helps resolve some of the contradictions and uncertainties regarding the previously proposed relative ice-flow chronologies and resulting dispersal patterns. Below, we discuss the timing of each ice-flow phase within the study area to allow for an understanding of larger-scale ice sheet dynamics. We use the data presented in this publication, as well as a detailed analysis of the surficial geologic record in the northern quarter of the study area (Rice et al., 2019, 2020c) to discuss the changing subglacial regimes and effects on glacial transport in the study area.

Flow 1 likely occurred after the last interglacial (Marine Isotope Stage (MIS) 5e (~123 ka)) as suggested by relatively low ^{10}Be abundances from outcrops within the Flow 1 landscape (i.e. limited to no inheritance; Rice et al., 2019). This is also supported by relatively low chemical index of alteration (CIA) values from till matrix geochemistry samples collected in the northern quarter of the study area (Rice et al., 2020c). The CIA values in this area (avg. 50) are significantly lower than CIA values correlated to regions of sustained cold-based conditions on Baffin Island (i.e. >70; Refsnider and Miller, 2010), suggesting there was sufficient subglacial erosion to remove the preglacial weathering signal in the Flow 1 landscape. If Flow 1 was from an older glacial event (i.e. pre-MIS 5e), bedrock outcrops with Flow 1 evidence should have higher ^{10}Be inheritance and in nearby till, higher CIA values. This hypothesis is supported by observations of an early northeast ice-flow phase identified in the surrounding regions (i.e. Klassen and Thompson, 1993; Veillette et al., 1999) and the broad evidence of Flow 1 across the majority of the study area, which taken together suggests Flow 1 was an extensive warm-based ice-flow phase that must have occurred while the Quebec-Labrador Dome was quite thick, possibly during LGM (MIS 2), and was not likely a pre-LGM flow (*cf.,* Klassen and Thompson, 1993; Veillette et al., 1999; Jansson et al., 2002; Clarhäll and Jansson, 2003). Glacial dispersal during Flow 1 is difficult to evaluate due to reworking and re-entrainment during subsequent ice-flow phases, however, certain patterns are still discernable. Trace elements, indicator minerals and clasts that are characteristic of the Labrador Trough (Cu, Sb, goethite, and iron formation clasts) show evidence of northeast dispersal, with iron formation clasts having been transported over 75 km from the bedrock source. Klassen and Thompson (1993) attributed northeast dispersal patterns with significant transport distances (up to 100 km from the bedrock source) to their earliest ice-flow phase (Event I). The dispersal of iron formation clasts over such a long distance somewhat conflicts with Rice et al. (2020c) who reported a transition to less erosive conditions in the central uplands (De Pas Batholith- Fig. 2), suggesting lower bed mobility and, theoretically, shorter dispersal distances. The development of these large dispersal fans over a low erosion zone suggests that, although the bedrock geology of the central uplands was more resistant to glacial erosion than other bedrock units, glacial dispersal was not impeded completely, allowing for long distance transport to occur. The mechanisms involved in long glacial transport over a portion of a low erosion subglacial bed under steady state glacial conditions remain enigmatic although may be related to reduced abrasion over hard beds (Alley et al., 2019), or glacial ripping of large bedrock blocks along bedrock fractures (Hall et al., 2020).

Following Flow 1, ice began to flow to the northwest (Flow 2), influenced by ice streaming into Ungava Bay. Northwest dispersal patterns of orthopyroxene grains and felsic intrusive clasts provide evidence of northwest glacial transport in the Lac Champdoré area resulting from Flow 2. Dispersal evidence to the northwest is limited elsewhere, as there was limited basal sliding occurring near and under a cold-based ice divide somewhere in the northeast of the study area (Fig. 19). Southeast dispersal correlated to Flow 2 is more difficult to assess due to the overprinting by later ice-flow phases within the Smallwood Reservoir area (e.g. Fig. 10). Klassen and Thomson (1993) attributed northwest dispersal of the Martin Lake rhyolite (Fig. 5) to their Event III toward Ungava Bay (our Flow 2). The dispersal

pattern of these clasts also has a dispersal component to the southeast (see Fig. 20 -Klassen and Thompson, 1993), which they attributed to the be the result of ice divide migration across the bedrock source, similar to the ice divide migration between Flow 2 and Flow 3 within our study area.

As the ice divide migrated west, ice began to flow east during Flow 3 in a nearly opposite direction to Flow 2, at least for the northwestern part of the study area. The activation of the CLIS in the study area during Flow 3 (Paulen et al., 2019a; Rice et al., 2020d) is associated with the early off-shore recession of the LIS and interpreted to have occurred contemporaneously with other ice streams flowing toward the Labrador coast (red arrows -Fig. 13). This transition from Flow 2 to Flow 3 appears to mark the boundary of the eastern arm of the U-shaped unconformity, suggesting the U-shaped boundary reflects changing subglacial thermal conditions, whereby warm-based ice formed northwest landforms toward Ungava Bay and were then preserved under more cold-based subglacial conditions as the ice divide migrated west. When the ice divide was positioned completely west of the study area, east-trending landforms developed under warm-based conditions during Flow 3. These varying basal thermal conditions are supported by the more detailed investigation of subglacial conditions in the northern part of the study area (Rice et al., 2020c).

Flow 3 reworked and re-entrained Flow 1 dispersal patterns and created palimpsest glacial dispersal patterns across the centre of the study area (e.g. Fig. 20). Regions where Flow 1 dispersal fans were reworked are greatest in areas where Flow 3 has the most predominant surficial signature (i.e. the highest abundance of east-trending landforms) as shown by the distribution of Cu from the Doublet Zone, which indicates Flow 3 has reworked Flow 1 dispersal to the northeast and re-entrained this material preferentially to the east (Fig. 16). Additional dispersal to the east associated with Flow 3 is observed in the dispersal of orthopyroxene grains and felsic clasts from the De Pas Batholith. Eastward dispersal was attributed by Klassen and Thompson (1993) to their Event II and in some cases Event IV. The absence of Martin Lake rhyolite clasts within the study area (Rice et al., 2020b), indicates this unique bedrock lithology was not dispersed as far as the iron formation clasts to the east or northeast and suggests that Martin Lake lithologies breakdown and weather more easily than resilient iron formation clasts.

As ice streaming continued to drain ice from the LIS, the profile of the ice sheet began to lower, leading to more topographic control on ice flows. Within the study area, this is observed by patterns associated with Flow 4 striations. Flow 4 was to the south in the west-central part of the study area, bounded by the central uplands to the east. Beyond the southern limit of these central highlands, the ice then continued to flow southeast into the Smallwood Reservoir (Fig. 12). Glacial dispersal patterns that result from this ice-flow phase are less pronounced than those formed by Flows 1, 2, and 3, likely due to the absence of a distinct geochemical, indicator mineral, or clast lithological signature within the confines of the ice-flow extent. However, given the abundance of landforms within its footprint, it is highly likely that Flow 4 remobilized and re-entrained existing dispersal patterns. Southeast dispersal from the Labrador Trough towards the Smallwood Reservoir is observed for Cu and iron formation clasts, and to a lesser degree, orthopyroxene grains from the western orthogneiss, although the patterns probably reflect early Flow 2 (to the south), or Flow 3 (to the east), or a combination of all three flows.

Dispersal patterns related to the youngest ice-flow events regrouped into Flow 5 were not observed. Glacial transport was likely minimal, as the ice sheet had thinned and further separated into regions of independent ice flow, with ice flow largely influenced by topography, although the ice-flow phase was generally to the northeast. Additionally, only poorly-developed streamlined landforms in a small low-lying area were identified related to this last ice-flow phase, indicating that it was characterized by relatively low erosion and hence had minimal impact on glacial sediment dispersal.

Deglaciation

Deglaciation of the area, as based on our OSL dating and ^{10}Be exposures ages, and constrained using regionally reported ^{10}Be ages, occurred by ~ 8 ka (Carlson et al., 2007, 2008; Ullman et al., 2016; Dubé-Loubert et al., 2018). Although ^{10}Be samples with relatively high levels of inheritance (moderate ^{10}Be abundances based on regional deglacial timing) are easily identified, those with low inheritance cannot be confidently recognized. Therefore, samples that are only centuries or even a millennium too old will be impossible to identify in the absence of complementary dating (e.g. ^{14}C) of morphostratigraphic controls (i.e. dating landforms that determine ice margin positions). Because our geochronological transect is devoid of end moraines, we have no such control on the amount of inheritance within our ^{10}Be samples. Furthermore, even if our younger ^{10}Be ages may represent maximum ages, averaging of regional ages is inappropriate. However, when the ^{10}Be ages and OSL dates are examined together (see Rice et al., 2019), our overall findings support previous work (Ives, 1960a; Clark et al., 2000) stating the Quebec-Labrador sector was highly fragmented in its late stages and disappeared by ~ 8 ka. They also correlate well with the more recent regional radiocarbon-based deglacial chronology presented by Dalton et al. (2020). In turn, our data suggest the U-shape boundary, at least at its southeastern extent, developed well before the formation of glacial lakes and therefore had no bearing on ice margin retreat patterns. However, we use topography (DEM data), identification of moraines, geomorphology and the position of moraines, meltwater channels, deglacial ages (OSL), and raised beach ridges to interpret ice margin retreat patterns and propose five general phases of glacial lake evolution for the study area. Figure 22 shows a generalized illustration of these phases presented in relative chronological order.

The glacial lake in the southeast of the study area was formally named glacial Lake Low during this research project (Paulen et al., 2017). Lake Low formed in the lowland region previously occupied by Lakes Ossokmanuan, Lobstick and Michikamau, and now occupied by the Smallwood Reservoir (Fig. 22A). The glacial lake formed as meltwater began to pond in the lowlands, constrained to the south by a drainage divide that must have been somewhere near the headwaters of the Churchill River (Paulen et al., 2020a, b; Fig. 22). A re-entrant extending from the headwaters of the Churchill River into the lowlands now occupied by the Smallwood Reservoir would allow the occurrence of an ice-free basin hosting Lake Low after 9.0 ka (OSL age-14-PTA-R035; Table 2). This glacial lake required an ice dam blocking the bedrock valleys, or fjords to the east of the study area, to prevent drainage to the Labrador coast. Lake Low formed and subsequently drained prior to northwestward ice margin retreat over the highlands to the north and west (Fig. 22).

As the ice sheet margin retreated north and west, meltwater accumulated in the headwaters of the George River valley, north of the paleo-drainage divide, which resulted in the formation of glacial Lake Naskaupi (Fig. 22B). Within our study area, two samples providing chronology on the maximum (15-PTA-149; elev. 486 ± 5 m) and minimum (15-PTA-074; elev. 314 ± 5 m) levels of Lake Naskaupi yielded ages of 7.93 ± 0.72 and 7.65 ± 0.99 ka, respectively (Fig. 22B and 22E). As the ice sheet thinned and further fragmented, Lake McLean developed in the lowlands of the Lac Champdoré area and formed beaches at 464 ± 5 m (Fig. 22D). However, our OSL sample collected from a beach of Lake McLean yielded an improbably old age (35.5 ± 4.0 ka), therefore the timing of this lake remains poorly constrained. DEM data suggest that Lake McLean must have formed when ice was blocking the De Pas River valley which prevented the lake from draining southeast into a lower phase of Lake Naskaupi.

As the ice continued to melt, overflow channels formed, before Lake Naskaupi catastrophically drained as indicated from evidence reported to the north of the study area (Dubé-Loubert and Roy, 2017). Following the catastrophic drainage of Lake Naskaupi N2 lake level (Dubé-Loubert et al., 2018),

a much lower Lake Naskaupi lingered in the George and De Pas River valleys at ~ 410 m (Fig. 22E). Glaciofluvial terraces, outwash fans, and the termini of meltwater channels were formed at this time. Sample 15-PTA-071, which was collected from an outwash fan terrace on the bank of the George River, indicated a depositional age of 7.65 ± 0.99 ka. This outwash fan is related to Lake Naskaupi at its lowest stage within the study area as do shorelines and terraces around this elevation (400 m) identified during surficial mapping (Rice et al., 2017a; Paulen et al., 2020b, 2020c). The timing of Lake McLean drainage is unknown, but it likely drained to the northwest along the Rivière à la Baleine valley (Fig. 4) based on available DEM data. Additional OSL ages are required to constrain the timing and paleogeographic reconstruction presented in Figure 22 and higher resolution DEM data would help constrain the overflow or drainage channels. The OSL results on samples of well-sorted sands (e.g. 15-PTA-074) yielded better results than those collected from more poorly-sorted sediments (e.g. 15-PTA-052). Thus, samples from lower energy environments with more consistent depositional rates should be favoured for OSL sampling, likely because these environments were less turbid and more readily exposed to sunlight.

SUMMARY

This work established five ice-flow phases with updated chronological constraints from landform and outcrop-scale ice-flow indicators. An early flow to the northeast (Flow 1), from an outflow centre somewhere in the Laurentian Highlands, was followed by the development or migration of an ice divide into the eastern half of the study area and a northwest ice-flow phase (Flow 2) highly influenced by ice stream dynamics in Ungava Bay. Changing dynamics in Ungava Bay led to the westward migration of the ice stream source areas and the concurrent westward migration of the ice divide across our study area, resulting in a more widespread eastward flow (Flow 3). Flow 3 is correlated with numerous ice streams generally flowing to the east that operated within and just outside of the study area. As the ice sheet continued to thin, ice began to flow south (Flow 4), topographically restricted by the central uplands, and feeding into the lowlands where the Smallwood Reservoir Ice Stream flowed to the east-southeast. Continued ice streaming led to significant ice sheet thinning that resulted in the youngest ice-flow phase eventually controlled by fragmented ice caps (Flow 5). As the ice margin retreated during deglaciation, three proglacial lakes formed within the study area. The earliest (and previously unmapped) Lake Low formed in the southeast, followed by continued ice margin retreat and the formation of Lake Naskaupi in the northeast and Lake McLean in the northwest. These lakes were identified by raised beaches and were targeted for OSL sampling that yielded deglacial ages that correlate with ^{10}Be exposure ages and indicate the region was deglaciated ~ 8000 years ago.

From this work, it is clear that the U-shaped boundary between glacially streamlined landforms is the result of contrasting and changing subglacial thermal conditions as reflected by the various preservation of landforms on either side, linked to ice divide migration across the region. As a result of the changing ice-flow patterns and subglacial thermal regimes, glacial dispersal patterns in the area are complex. Our work shows that dispersal patterns are largely the result of broad northeast dispersal during Flow 1, reworked by subsequent ice-flow phases restricted to more localized regions. It also expands the range of previously documented iron formation erratic dispersal to the northeast by 50 km. Additionally, the conflicting ice-flow chronologies for the region have been resolved, at least within the study area, providing a framework for reconstructing regional ice-flow phases and for interpreting glacial transport with applications to mineral exploration. The timing and pattern of ice margin retreat have also been refined; however, additional age data would improve the accuracy and resolution of the proposed reconstruction. Overall, this research has provided important insights into the changing subglacial conditions within the inner regions of large ice sheets throughout glaciation.

ACKNOWLEDGEMENTS

The Core Zone surficial research activity was carried out as part of the Hudson-Ungava Project under the GSC's GEM2 Program in collaboration with the Ministère de l'Énergie et des Ressources naturelles du Québec (MERNQ) and the Geological Survey of Newfoundland and Labrador. It was ably managed by Réjean Couture, Lila Chebab, and Jennifer Bates, with support from Daniel Sincennes and Ryan Murphy. The GSC provided financial support to the first author in the form of a bursary through the Research Affiliate Program. Logistical support for field activities was expertly provided by the Polar Continental Shelf Program (Project #059-15 and #060-16) and Norpaq Aviation. The authors thank Matt Pyne (GSC Ottawa) and Gabriel Huot-Vézina (GSC Quebec) for GIS and database support. Assistance in the field was provided by Grant Hagedorn (University of Waterloo), Alan Lion (University of Ottawa), and Emilie Rufiange (University of Ottawa). Samuel Kelley (University College Dublin) and Jason Briner (University at Buffalo) are thanked for their assistance with ^{10}Be interpretation. We are grateful to David Corrigan and Mary Sanborn-Barrie (GSC Ottawa) for their insights and assistance with related aspects of the bedrock geology. Alan Rioux and Maxim Gauthier (Innokopters Inc.) are thanked for safe transportation and assistance in the field. Pierre-Marc Godbout, Jean Veillette, and Arthur Dyke provided thoughtful comments that greatly improved this manuscript. Isabelle McMartin is thanked for her very hard work as editor of this volume and valuable feedback on this publication.

REFERENCES

Aitken, M.J., 1998. An Introduction to Optical Dating, Oxford University Press, 267 p.

Allard, M., Fournier, A., Gahé, E., and Séguin, M.K., 1989. Le Quaternaire de la côte sud-est de la baie d'Ungava, Québec nordique; Géographie physique et Quaternaire, v. 43, p. 325-336.

Alley, R.B., Cuffey, K.M., and Zoet, L.K. 2019. Glacial erosion: status and outlook. Annals of Glaciology 1-13. doi: 10.1017/aog.2019.38

Amor, S., McCurdy, M., and Garrett, R., 2019. Creation of an atlas of lake-sediment geochemistry of western Labrador and northeastern Québec; Geochemistry: Exploration, Environment, Analysis, v.19, p. 369-393. doi: 10.1144/geochem2018-061

Argus, D.F., Peltier, W.R., Drummond, R., and Moore, A.Q., 2014. The Antarctica component of postglacial rebound model ICE- 6G_C (VM5a) based upon GPS positioning, exposure age dating of ice thicknesses, and relative sea level histories; Geophysics Journal International, v. 198, p. 537-563.

Barnett, D.M., 1967. Glacial Lake McLean and its relationship with Glacial Lake Naskaupi; Geographical Bulletin, v.9 p. 96-101.

Barnett, D.M. and Peterson, J.A., 1964. The significance of glacial Lake Naskaupi 2 in the deglaciation of Labrador- Ungava; The Canadian Geographer, v. 8, p. 173-181.

Bostock, H.S., 2014. Physiographic regions of Canada; Geological Survey of Canada, "A" series Map 1254A, 1: 5 000 000 scale. doi: 10.4095/293408

Brouard, E. and Lajeunesse, P., 2019. Ice-stream flow switching by up-ice propagation of instabilities along glacial marginal troughs; The Cryosphere, v. 13, p. 198-996.

Brushett, D. and Amor, S., 2013. Kimberlite-indicator mineral analysis of eskers samples, western Labrador; Government of Newfoundland and Labrador, Department of Natural Resources, Open File LAB/1620.

Campbell, H.E., Paulen, R.C., and Rice, J.M., 2018. Surficial geology, Ashuanipi River, Newfoundland and Labrador, NTS 230I southwest. Geological Survey of Canada, Canadian Geoscience Map 346, scale 1: 100 000, 1. doi: 10.4095/306431

Carlson, A.E., Clark, P.U., Raisbeck, G.M., and Brook, E.J., 2007. Rapid Holocene deglaciation of the Labrador sector of the Laurentide Ice Sheet; Journal of Climate, v. 20, p. 5126-5133.

Carlson, A.E., LeGrande, A.N., Oppo, D.W., Came, R.E., Schmidt, G.A., Anslow, F.S., Licciardi, J.M., and Obbink, E.A., 2008. Rapid early Holocene deglaciation of the Laurentide Ice Sheet; Nature Geoscience, v. 1, p. 620-624.

Clarhäll, A. and Jansson, K., 2003. Time perspectives on glacial landscape formation – glacial flow chronology at Lac aux Goélands, northeastern Québec, Canada; Journal of Quaternary Science, v. 18, no. 5, p. 441-452.

Clark, C.D., Knight, J.K., and Gray, J.T., 2000. Geomorphological reconstruction of the Labrador Sector of the Laurentide Ice Sheet; Quaternary Science Reviews, v. 19, p. 5126-5133.

Clark, P.U. and Fitzhugh, W.W., 1990. Late Deglaciation of the central Labrador coast and its implications for the age of Glacial lakes Naskaupi and McLean and for prehistory; Quaternary Research, v. 34, no. 3, p. 296-305.

Clark, P.U., Brook, E.J., Raisbeck, G.M., Yiou, F., and Clark, J., 2003. Cosmogenic ^{10}Be ages of the Saglek Moraines, Torngat Mountains, Labrador; Geology, v. 31, p. 617-620.

Clark, T. and Wares, M., 2005. Lithotectonic and metallogenic synthesis of the New Québec Orogen (Labrador Trough); Ministère des Ressources naturelles du Québec, MM 2005-01, 175 pages.

Corrigan, D., Van Rooyen, D., Morin, A., Houlé, M.G., and McNicoll, V.J., 2015. Report of activities for the Core Zone and bounding orogens: The New Quebec Orogen and its relationship with the Core Zone in Kuujjuaq area; Geological Survey of Canada, Open File 7962, 1 .zip file. doi: 10.4095/297404

Corrigan, D., van Rooyen, D., Morin, A., Houlé, M.G., and Bédard, M-P. 2016. Report of activities for the Core Zone and bounding orogens: Recent observations from the New Quebec Orogen in the Schefferville area, Quebec and Labrador; Geological Survey of Canada, Open File 8127.

Corrigan, D., Wodicka, N., McFarlane, C., Lafrance, I., van Rooyen, D., Bandyayera, D., and Bilodeau, C., 2018. Lithotectonic framework of the Core Zone, southeastern Churchill Province, Canada; Geoscience Canada, v. 45, p. 1-24. doi: 10.12789/geocanj2018.45.128

Cowan, W.R., 1967: The glacial geomorphology of the Shoal Lake area, Labrador; Unpublished M.Sc. thesis, McGill University, Montréal, 127 p.

Dalton, A.S., Margold, M., Stokes, C.R., Tarasv, L. et al., 2020. An updated radiocarbon-based ice margin chronology of the last deglaciation of the North American Ice Sheet Complex; Quaternary Science Reviews, v. 234, p. 106-223. doi: 10.1016/j.quascirev.2020.106223

Douglas, M.C.V., and Drummond, R.N., 1955. Map of the Physiographic regions of Ungava-Labardor. The Canadian Geographer, v. 2, p. 9-16. doi : 10.1111/j.1541-0064.1955.tb01746.x

Dubé-Loubert, H., 2019. Dynamique glaciaire et géochronologie du secteur Labrador de l'lnlandsis laurentidien et évolution du lac Naskaupi au cours de la dernière déglaciation. Ph.D. thesis, Université du Québec à Montréal, Montreal, Québec, 179 p.

Dubé-Loubert, H. and Roy, M., 2017. Development, evolution and drainage of glacial Lake Naskaupi during the deglaciation of north-central Quebec and Labrador; Journal of Quaternary Science, v. 32, p. 1121-1137.

Dubé-Loubert, H., Roy, M., Schaefer, J.M., and Clark, P.U., 2018. ^{10}Be dating of former glacial Lake Naskaupi (Québec-Labrador) and timing of its discharges during the last deglaciation; Quaternary Science Reviews, v. 191, p. 31-40.

Dunai, T.J., 2010. Cosmogenic Nuclides: Principals, Concepts, and Applications in Earth Surface Sciences; Cambridge University Press, 198p.

Dyke, A.S., 2004. An outline of North American deglaciation with emphasis on central and northern Canada; *in* Quaternary glaciations — extent and chronology, Part II. North America, (eds.) J. Ehlers and P.L. Gibbard; Elsevier B.V., Amsterdam, Development in Quaternary Science Series, p. 371-406.

Dyke, A.S. and Prest, V.K., 1987. Late Wisconsinan and Holocene history of the Laurentide Ice Sheet; Géographie physique et Quaternaire, v. 2, p. 237-263.

Dyke, A.S., Dredge, L.A., and Vincent, J-S., 1982. Configuration and Dynamics of Laurentide Ice Sheet during the Late Wisconsin Maximum. Géographie Physique et Quaternaire, v. 36, p. 5-14. doi: 10.7202/032467ar

Dyke, A.S., Morris, T.F., Green, D.E.C., and England, J.,1993. Quaternary geology of Prince of Wales Island, Arctic Canada. Geological Survey of Canada Memoir 433. doi 10.4095/134058

Fuchs, M. and Owen, L.A., 2008. Luminescence dating of glacial and associated sediment: review, recommendations and future directions; Boreas, v. 37, p. 636-659

Fulton, R.J., 1995. Surficial materials of Canada; Geological Survey of Canada "A" Series Map no. 1880A, scale, 1:5 000 000 scale. doi: 10.4095/295462

Fulton, R.J., and Hodgson, D.A., 1979. Wisconsin glacial retreat, southern Labrador. Geological Survey of Canada Current Research, Part C. doi: 10.4095/124066

Gauthier, M.S., Hodder, T.J., Ross, M., Kelley, S.E., Rochester, A., and McCausland, P., 2019. The subglacial mosaic of the Laurentide Ice Sheet; a study of the interior region of southwestern Hudson Bay; Quaternary Science Reviews, v. 214, p. 1-27.

Gowan, E.J., Niu, L., Knorr, G., and Lohmann, G. 2019. Geology datasets in North America, Greenland and surrounding areas for use with ice sheet models; Earth System Science Data, v. 11, p. 375-391. doi: 10.5194/essd-11-375-2019

Granberg, H.B. and Krishnan, T.K., 1984. Wood remnants 24,250 years old in central Labrador (abstract); *in* Program and Abstracts, 5th AQQUA Congress, Sherbrooke, p. 30.

Hall, A.M., Krabbendam, M., van Boeckel, M., Goodfellow, B.W., Hätterstrand, C., Heyman, J., Palamakumbura, R.N., Stroeven, A.P., and Näslund, J-O., 2020. Glacial ripping: geomorphological evidence from Sweden for a new process of glacial erosion. Geografiska Annaler: Series A, Physical Geography, 102 (4), 333-353. doi: 10.1080/04353676.2020.1774244

Henderson, E.P., 1959. A glacial study of central Quebec-Labrador; Geological Survey of Canada, Bulletin 50, 94p. doi: 10.4095/123901

Hickin, A.S., Lian, O.V., Levson, V.M., and Cui, Y., 2015. Pattern and chronology of glacial Lake Peace shorelines and implications for isostasy and ice-sheet configuration in northeastern British Columbia, Canada; Boreas, v. 44, p. 228-304.

Hillaire-Marcel, C., Occhietti, S., and Vincent, J-S., 1981. Sakami moraine, Quebec: A 500-km long moraine without climatic control. Geology, v. 9(5), p. 210-214. doi: 10.1130/0091-7613(1981)<210:SMWAKM>2.0.CO;2

Huntley, D.J. and Lamothe, M., 2001. Ubiquity of anomalous fading in K-feldspars and the measurements and correction for it in optical dating. Canadian Journal of Earth Science, v. 38, p. 1093-1106. doi: 10.1139/e01-013

Hughes, O.L., 1964. Surficial Geology, Nichicun-Kaniapiskau Map-Area, Quebec. Geological Survey of Canada; Bulletin 106. doi: 10.4095/100624

Ives, J., 1956. Till patterns in Central Labrador. Canadian geographer, v. 8,p. 25-33.

Ives, J.D., 1958. Glacial drainage channels as indicators of Late-glacial conditions in Labrador-Ungava: a discussion; Cahiers de Géographie due Québec, v.3, p. 57-72.

Ives, J.D., 1960a. The deglaciation of Labrador-Ungava- An outline; Cahiers de Géographie du Québec, v. 4, p. 323-343.

Ives, J.D., 1960b. Former ice-dammed lakes and the deglaciation of the middle reaches of the George River, Labrador-Ungava; Geographical Bulletin, v. 14, p. 44-69.

James, D.T., Johnston, D.H., and Crisby-Wittle, L., 1993. Geology of the eastern Smallwood Reservoir area, western Labrador; *in* Current Research, Newfoundland Department of Mines and Energy, Geological Survey Branch, Report 93-1, p. 35-49.

James, D.T., Connelly, J.N., Wasteneys, H.A., and Kilfoil, G.J., 1996. Paleoproterozic litholotectonic divisions of the southeastern Churchill Province, western Labrador; Canadian Journal of Earth Sciences, v. 33, p. 216-230. doi: 10.1139/e96-019

James, D.T., Nunn, G.A.G., Kamo, S., and Kwok, K., 2003. The southeastern Churchill Province revisited: U-Pb geochronology, regional correlations, and enigmatic Orman Domain; Newfoundland Department of Mines and Energy, Current Research 03-1, pp. 35-45.

Jansson, K.N., 2005. Map of the glacial geomorphology of north-central Québec-Labrador, Canada. Journal of Maps, v. 1(1), p. 46-55.

Jansson, K.N., Kleman, J., and Marchant, D.R., 2002. The succession of ice-flow pattern in north central Quebec-Labrador, Canada; Quaternary Science Review, v.21, p. 503-523.

Jansson, K.N., Stroeven, A.P., and Kleman, J., 2003. Configuration and timing of Ungava Bay ice streams, Labrador-Ungava, Canada; Boreas, v. 32, p. 256-262.

Kirby, R.P., 1962. Movements of ice in Central Labrador-Ungava; Cahiers de Géographie du Québec, v. 5, p. 206-218.

Klassen, R.A. and Bolduc, A.M., 1984. Ice flow directions and drift composition, Churchill Falls, Labrador; Current Research, Geological Survey of Canada, Part A, 84-1A, p. 255-258.

Klassen, R.A. and Knight, R.D., 1995. Till geochemistry of central Labrador; Geological Survey of Canada, Open File 3213, 250p.

Klassen, R.A. and Thompson F.J., 1987. Ice flow history and glacial dispersal in the Labrador Trough; Geological Survey of Canada, Current Research Part A, Paper no. 87-1A, p. 61-710.

Klassen, R.A. and Thompson, F.J., 1988. Glacial studies in Labrador; Geological Survey of Canada, Current Research Part C, Paper No. 88-1C, p. 109-116.

Klassen, R.A. and Thompson, F.J., 1989. Ice flow history and glacial dispersions, Labrador; *in* Drift Prospecting, (eds.) R.N.W., DiLabio and W.B., Coker, Geological Survey of Canada, Paper 89-20, p. 21-29.

Klassen, R.A., and Paradis, S., 1990. Surficial geology of western Labrador. Geological Survey of Canada, Open File 2198. doi: 10.4095/130817

Klassen, R.A. and Thompson, F.J., 1993. Glacial history, drift composition, and mineral exploration, central Labrador; Geological Survey of Canada, Bulletin 435. Doi: 10.4095/183906

Klassen, R.A., Matthews, J.V.J., Mott, R.J., and Thompson, F.J., 1988. The stratigraphic and paleobotanical record of interglaciation in the Wabush region of western Labrador (abstract); *in:* Climatic Fluctuations and Man 3, Annual Meeting of the Canadian Committee on Climatic Fluctuations, Jan. 18-19, 1988 Ottawa: 22-26.

Klassen, R.A., Paradis, S., Bolduc, A.M., and Thomas, R.D., 1992. Glacial landforms and deposits, Labrador, Newfoundland and eastern Québec; Geological Survey of Canada, A Series Map 1814A, 1: 1 000 000 scale. Geoscan ID: 183872. doi: 10.4095/183872

Kleman, J. and Glasser, N.F. 2007. The subglacial thermal organisation (STO) of ice sheets. Quaternary Science Reviews, 26: 585-597.

Kleman, J., Fastook, J., and Stroeven, A.P. 2002. Geologically and geomorphologically constrained numerical model of Laurentide Ice Sheet inception and build-up. Quaternary International, 95: 87-98.

Lal, D., 1991. Cosmic ray labeling of erosion surfaces: in situ nuclide production rates and erosion models. Earth and Planetary Science Letters, v. 104, p. 424-439.

Lauriol, B. and Gray, J.T., 1987. The Decay and Disappearance of the Late Wisconsin Ice Sheet in the Ungava Peninsula, Northern Quebec, Canada; Arctic and Alpine Research, v. 19, n. 2, p. 109-126.

Lepper, K., Buell, A.W., Fisher, T.G., and Lowell, T.V., 2013. A chronology for glacial Lake Agassiz along Upham's namesake transect; Quaternary Research, v. 80, p. 88-98.

Lifton, N., Sayo, T., and Dunai, T.J., 2014. Scaling in situ cosmogenic nuclide production rates using analytical approximations to atmospheric cosmic-ray fluxes; Earth and Planetary Science Letters, v. 386, p. 149-160.

Liverman, D. and Vatcher, H., 1992. Surficial geology of the Cavers and Hollinger Lake areas (NTS 23J/9 and 16); *in* Current Research, Government of Newfoundland and Labrador, Department of Mines and Energy, Geological Survey Branch, Report 93-1, p. 127-138.

Liverman, D. and Vatcher, H., 1993. Surficial geology of the Schefferville area (Labrador parts of NTS 23J/10 and 23J/15; *in* Current Research, Government of Newfoundland and Labrador, Department of Mines and Energy, Geological Survey Branch, Report 92-1, p. 27-37.

Low, A.P., 1896. Report on explorations in the Labrador Peninsula along the Eastman, Koksoak, Hamilton, Manikuagan and portions of other rivers in 1892-93-94-95; Geological Survey of Canada, Annual Report, Volume 8, Part L.

Margold, M., Stokes, C.R., Clark, C.D., and Kleman, J., 2015. Ice streams in the Laurentide Ice Sheet: a new mapping inventory; Journal of Maps, v. 11, p. 180-395. doi: 10.1080/17445647.2014.912036

Margold. M., Stokes, C.R., and Clark, C.D., 2018. Reconciling records of ice streaming and ice margin retreat to produce a paleographic reconstruction of the deglaciation of the Laurentide Ice Sheet; Quaternary Science Reviews, v. 189, p. 1-30.

Marquette, G.C., Gray, J.T., Gosse, J.T., Courchesne, F., Stockli, L., Macpherson, G., and Finkle, R., 2004. Felsenmeer persistence under non-erosive ice in the Torngat and Kaumajet mountains, Quebec and Labrador, as determined by soil weathering and cosmogenic nuclide exposure dating; Canadian Journal of Earth Sciences, v. 41, p. 19-38.

Mathewes, R.W., Lian, O.B., Clague J.J., and Huntley M.J.W., 2015. Early Wisconsinan (MIS 4) glaciation on Haida Gwaii, British Columbia, and implications for biological refugia; Canadian Journal of Earth Science, v. 52, p. 939-951.

Matthews, B., 1961. Late Quaternary land emergence in northern Ungava, Quebec. Arctic, v. 20, p. 176-202.

McClenaghan, M.B., Plouffe, A., McMartin, I., Campbell, J.E., Spirito, W.A., Paulen, R.C., Garrett, R.G., and Hall, G.E.M., 2013. Till sampling and geochemical analytical protocols used by the Geological Survey of Canada; Geochemistry: Exploration, Environment, Analysis, v.13, p. 285-301.

McClenaghan, M.B., Paulen, R.C., Rice, J.M., Pyne, M., and Lion, A., 2016a. Till geochemical data for the south Core Zone, Quebec and Labrador (NTS 23-P and 23-I): till samples collected in 2014; Geological Survey of Canada, Open File 7967, 32 p. doi: 10.4095/297796

McClenaghan, M.B., Paulen, R.C., and Rice, J.M., 2016b. Indicator mineral abundance data for till samples from the south Core Zone, Quebec and Labrador (NTS 23-P and 23-I): samples collected in 2014; Geological Survey of Canada, Open File 7968, 1 .zip file. doi: 10.4095/297379

McClenaghan, M.B., Paulen, R.C., Rice, J.M., Campbell, H.E., and Pyne, M.D., 2017. Gold grains in till samples from the southern Core Zone, Quebec and Newfoundland and Labrador (NTS 23-P and 23-I): potential for undiscovered mineralization; Geological Survey of Canada, Open File 8222, 1 .zip file. doi: 10.4095/300657

McClenaghan, M.B., Spirito, M.B., Plouffe, W.A., McMartin, A, Campbell, I., Paulen, R.C., Garrett, R.G., Hall, G.E.M., Pelchat, P., and Gautheir, M.S., 2020. Geological Survey of Canada till-sampling and analytical protocols: from field to archive, 2020 update. Geological Survey of Canada, Open File 8591. doi: 10.4095/326162

McMartin, I. and Paulen, R.P., 2009. Ice-flow indicators and the importance of ice-flow mapping for drift prospecting. *in* Application of till and stream sediment heavy mineral and geochemical methods to mineral exploration in western and northern Canada, (eds.) R.C. Paulen and I. McMartin (eds.). Geological Association of Canada, Short Course Notes 18, p. 15–34.

Melanson, A., Bell, T., and Tarasov, L. 2013. Numerical modelling of subglacial erosion and sediment transport and its application the North American ice sheets over the Last Glacial cycle. Quaternary Science Reviews, 68: 154-174. doi: 10.1016/j.quascirev.2013.02.017

Neal, H.E., 2000. Iron Deposits of the Labrador Trough. Exploration and Mining Geology, v. 8, p. 113-121. doi: 10.2113/0090113

Occhietti, S., Govare, É., Klassen, R., Parent, M., and Vincent, J-S., 2004. Late Wisconsin- Early Holocene deglaciation of Québec-Labrador. *in* Quaternary glaciations- extent and chronology, Part II. North America, (eds.) J. Ehlers and P.L. Gibbard, Elsevier B.V., Amsterdam, Development in Quaternary Science Series, p. 371-406.

Parent, M., Beaumier, M., Girard, R., and Paradis, S.J., 2004. Diamond exploration in the Archean craton of northern Quebec: Kimberlite indicator minerals in eskers of the Saidon-Cambrian corridor; Quebec Ministry of Natural Resources, Fauna and Parks, Manuscript 2004-02.

Paulen, R.C., Rice, J.M., and McClenaghan, M.B., 2015. Streamlined and lobate landforms, relating to successive ice flows in the Smallwood Reservoir, northern Labrador. [Poster] Joint Assembly AGU-GAC-MAC-CGU. Montreal, QC. May 2015.

Paulen, R.C., Rice, J.M., and McClenaghan, M.B., 2017. Surficial geology, northwest Smallwood Reservoir, Newfoundland and Labrador, NTS 23-I southeast; Geological Survey of Canada, Canadian Geoscience Map 315, scale 1: 100 000, 1 sheet. doi: 10.4095/300685

Paulen, R.C., Rice, J.M., and Ross, M., 2019a. Surficial geology, Adelaide Lake, Newfoundland and Labrador- Quebec, NTS 23-I northeast; Geological Survey of Canada, Canadian Geoscience Map 395, scale 1: 100 000, 1 sheet. doi: 10.4095/313655

Paulen, R.C., Rice, J.M., Campbell, H.E., and McClenaghan, M.B. 2019b. Surficial geology, Knox Lake, Newfoundland and Labrador-Quebec, NTS 23-I northwest. Geological Survey of Canada, Canadian Geoscience Map 377, scale 1: 100 000, 1 sheet. doi: 10.4095/313547

Paulen, R.C., Rice, J.M., Ross, M., and Lian, O.B. 2020a. Glacial Lake Low: a previously unidentified proglacial lake in western Labrador [abstract]. Geological Society of America Annual Meeting, Online, v. 2 (6). doi: 10.1130/abs/2020AM-358203.

Paulen, R.C., Rice, J.M., Ross, M., and Lian, O.B. 2020b. Timing and paleogeographic reconstruction of glacial Lake Low in western Labrador. Geoconvention 2020 (GAC-MAC-IAH-CNC-CSPG-CSEG-CWLS), Calgary 2020, conference paper, 4 p.

Paulen, R.C., Rice, J.M., and Ross, M., 2020c Surficial geology, Lac Laporte, Quebec, NTS 23-P southwest. Geological Survey of Canada, Canadian Geoscience Map 410, scale 1: 100 000, 1 sheet. doi: 10.4095/314756

Paulen, R.C., Rice, J.M., and Ross, M., 2022. Surficial geology, Lac aux Goélands, Quebec, NTS 23-P southeast. Geological Survey of Canada, Canadian Geoscience Map 429, scale 1: 100 000, 1 sheet. doi: 10.4095/1328291

Peltier, W.R., Argus, D.F., and Drummond, R., 2015. Space geodesy constrains ice age terminal deglaciation: The global Ice-6G_C (VM5a) model, Journal of Geophysical Research; Solid Earth, v. 120, p. 450-487.

Peterson, J.A., 1965. Deglaciation of the Whitegull Lake area, Labrador-Ungava; Cahiers de Géographie du Québec, v. 9, p. 183-196. doi: 10.7202/020596ar

Plouffe, A., McClenaghan, M.B., Paulen, R.C., McMartin, I., Campbell, J.E., and Spirito, W.A., 2013. Processing of unconsolidated glacial sediments for the recovery of indicator minerals: Protocols used at the Geological Survey of Canada; Geochemistry: Exploration, Environment, Analysis, v.13, p. 303-316.

Prest, V.K. 1970. Quaternary Geology of Canada; *in* Geology and Economic Minerals of Canada, Economic Geology Re. No.1. Geological Survey of Canada, p. 676-764.

Prichart, H.H., 1911. Through trackless Labrador- with a chapter on fishing by Gathorne-Hardy; Sturgis and Walton, New York, NY.

Refsnider, K.A. and Miller, G.H. 2010. Reorganization of ice sheet flow patterns in Arctic Canada and the mid-Pleistocene transition. Geophysical Research Letter, 37: 1-5.

Reyes, A., Dillman, T., Kennedy, K., Froese, D., Beaudoin, A.B., and Paulen, R.C., 2020. Legacy radiocarbon ages and the MIS 3 Dating Game: A cautionary tale form re-dating of Pre-LGM sites in Western Canada. Geological Society of America Connects online, Paper 56-36. doi: 10.1130/abs/2020AM-360064

Rice, J.M., McClenaghan, M.B., Paulen, R.C., Pyne, M.D., and Ross, M., 2017a. Till geochemical data for the southern Core Zone, Quebec and Newfoundland and Labrador (NTS 23-P and 23-I): samples collected in 2015 and 2016; Geological Survey of Canada, Open File 8219. doi: 10.4095/304280.

Rice, J.M., McClenaghan, M.B., Paulen, R.C., Ross, M., Pyne, M.D., and Lion, A. J., 2017b. Indicator mineral abundance data for till samples from the south Core Zone, Quebec and Labrador (NTS 23-P and 23-I): Samples collected in 2015; Geological Survey of Canada, Open File 8187. doi: 10.4095/299683

Rice, J.M., Paulen, R.C., and Ross, M., 2017c. Surficial geology, Rivière De Pas, Quebec, NTS 23-P northwest. Geological Survey of Canada, Canadian Geoscience Map 333, scale 1: 100 000, 1 sheet. doi: 10.4095/306166

Rice, J.M., Paulen, R.C., and Ross, M., 2017d. Surficial geology, Lac Mistinibi, Quebec, NTS 23-P northeast. Geological Survey of Canada, Canadian Geoscience Map 316, scale 1: 100 000, 1 sheet. doi: 10.4095/300656

Rice, J.M., Ross, M., Paulen, R.C., Kelley, S.E., Briner, J.P., Neudorf, C.M., and Lian, O. B., 2019. Refining the ice flow chronology and subglacial dynamics across the migrating Labrador Divide of the Laurentide Ice Sheet with age constraints on deglaciation; Journal of Quaternary Science, v. 34, p. 519-535. doi: 10.1002/jqs3138

Rice, J.M., McClenaghan, M.B., Paulen, R.C., Pyne, M.D. Ross, M., and Campbell, H.E. 2020a. Field data for till samples collected in 2014, 2015, and 2016 in the southern Core Zone, Quebec and Labrador (NTS 23-P and 23-I); Geological Survey of Canada, Open File 8655, 2020, 11 pages. doi: 10.4095/321471

Rice, J.M., Paulen, R.C., Ross, M., and McClenaghan, M.B. 2020b. Clast lithology data from the southern Core Zone, Quebec and Newfoundland and Labrador (NTS 23-I and 23-P), Geological Survey of Canada, Open File 8721, 14 pages. doi: 10.4095/326083

Rice, J.M., Ross, M., Paulen, R.C., Kelley, S.E., and Briner, J.P., 2020c. A GIS-based multi-proxy analysis of the evolution of subglacial dynamics in northeastern Quebec, Canada; Earth Surface Processes and Landforms, v. 23(13), p. 3155-3177. doi: 10.1002/esp.4957

Rice, J.M., Ross, M., and Paulen, R.C., 2020d. The Cabot Lake Ice Stream: a paleo-ice stream near the Ancestral Labrador ice divide of the Laurentide Ice Sheet's Quebec-Labrador dome; Geological Survey of Canada Scientific Presentation 109, 1 sheet. doi: 10.4095/321077

Ross, M., Campbell, J.E., Parent, M., and Adams, R.S., 2009. Paleo-ice streams and the subglacial mosaic of the North American mid-continental praries. Boreas, v. 38, p. 421-439. doi: 10.1111/j.1502-3885.2009.00082.x

Roy, M., Veillette, J., Daubois, V., and Ménard, M., 2015. Late-stage phases of glacial Lake Ojibway in the central Abitibi region, eastern Canada. Geomorphology, v. 248, p. 14-23.

Sanborn-Barrie, M., 2016. Refining lithological and structural understanding of the southern Core Zone, northern Quebec and Labrador in support of mineral resource assessment; Geological Survey of Canada, Open File 7956. doi: 10.4095/297560

Short, S.K., 1981. Radiocarbon date list I: Labrador and northern Quebec, Canada; Institution of Arctic and Alpine Research, Occasional Paper 36, p. 1-33.

Smith, S., 2010. Trends in permafrost conditions and the ecology in northern Canada; Canadian Biodiversity: Ecosystem Status and Trends 2010, Canadian Councils of Resource Ministers Technical Thematic Report No. 9.

Staiger, J.W., Gosse, J., Little, E.C., Utting, D.J., Finkel, R., Johnson, J.V., and Fastook, J. 2006. Glacial erosion and sediment dispersion from detrital cosmogenic nuclide analyses of till. Quaternary Geochronology, 1: 29-42.

Stone, J.O., 2000. Air pressure and cosmogenic isotope production. Journal of Geophysical Research, v. 105, p. 23753-23759.

Stokes, C.R. and Clark, C.D., 2001. Paleo-ice streams; Quaternary Science Reviews, v. 20, p. 1437-1457.

Stokes, C.R., Tarasov, L., and Dyke, A.S. 2012. Dynamics of the North American Ice Sheet Complex during its inception and build-up to the Last Glacial Maximum. Quaternary Science Reviews, 50: 86-104.

Tanner, V., 1948. Outlines of the geography, life and customs of Newfoundland-Labrador (The eastern part of the Labrador Peninsula); The Journal of Geology, v.56, p. 495-495. doi: 10.1086/625547

Tarasov, L. and Peltier, W.R. 2004. A geophysically constrained large ensemble analysis of the deglacial history of the North American ice-sheet complex. Quaternary Science Reviews, 23 (3-4): 359-388.

Ullman, D.J., Carlson, A.E., Anslow, F.S., LeGrande, A.N., and Licciardi, J.M. 2015. Laurentide ice-sheet instability during the last deglaciation; Nature Geoscience, v. 8, p. 534-537.

Ullman, D.J., Carlson, A.E., Hostetler, S.W., Clark, P.U., Cuzzone, J., Milne, G.A., Winsor, K., and Caffee, M., 2016. Final Laurentide ice-sheet deglaciation and Holocene climate-sea level change; Quaternary Science Reviews, v.152, p. 49-59.

van der Leeden, J., Belanger, M., Danis, D., Girad, R., and Martelain, J., 1990. Lithotectonic domains in the high-grade terrain east of the Labrador Trough, Quebec; *in* The Early Proterozoic Trans-Hudson Orogen of North America, (eds.) J.F., Lewry, and M.R., Stauffer, Geological Association of Canada, Special Paper 37, p. 371-386.

Veillette, J.J. and Roy, M., 1995. The spectacular cross-striated outcrops of James Bay, Quebec; Current Research No. 1995-C, Geological Survey of Canada, p. 243-248. doi: 10.4095/202923

Veillette, J.J., Dyke, A.S., and Roy, M., 1999. Ice-flow evolution of the Labrador Sector of the Laurentide Ice Sheet: a review, with new evidence from northern Quebec; Quaternary Science Reviews, v. 18, p. 993-1019. doi: 10.1016/S0277-3791(98)00076-6

Vincent, J-S. 1989. Quaternary geology of the southeastern Canadian Shield: In Chapter 3 of Quaternary Geology of Canada and Greenland, Fulton RJ (ed). Geological Survey of Canada, Geology of Canada, no.1.

Wallace, W.S., 1932. John McLean's notes of a 25 years service in Hudson's Bay Company Territory. Champlain Society Toronto 19, 402 p.

Wardle, R.J., 1982. Geology of the south-central Labrador Trough, Maps 82-5 and 82-6; Scale 1:100,000. Mineral Development Division, Department of Mines and Energy, Government of Newfoundland and Labrador.

Wardle, R.J., James, D.T., and Hall, J., 2002. The southeastern Churchill Province: synthesis of a Paleoproterozoic transpressional orogen; Canadian Journal of Earth Sciences, v. 39, p. 369-366.

Wilson, J.T., Drummond, R.N., and Douglas, M.C.V., 1953; Terrain Analysis Maps (air photo interpretation). Canada Defense Research Board, Ottawa.

Younge, N.E., Schaeffer, J.M., Briner, J.P., Goehring, B.M., 2013. A 10Be production-rate calibration for the Arctic. Journal of Quaternary Science, v. 28, p. 515-526. doi: 10.1002/jqs.2642

Figures

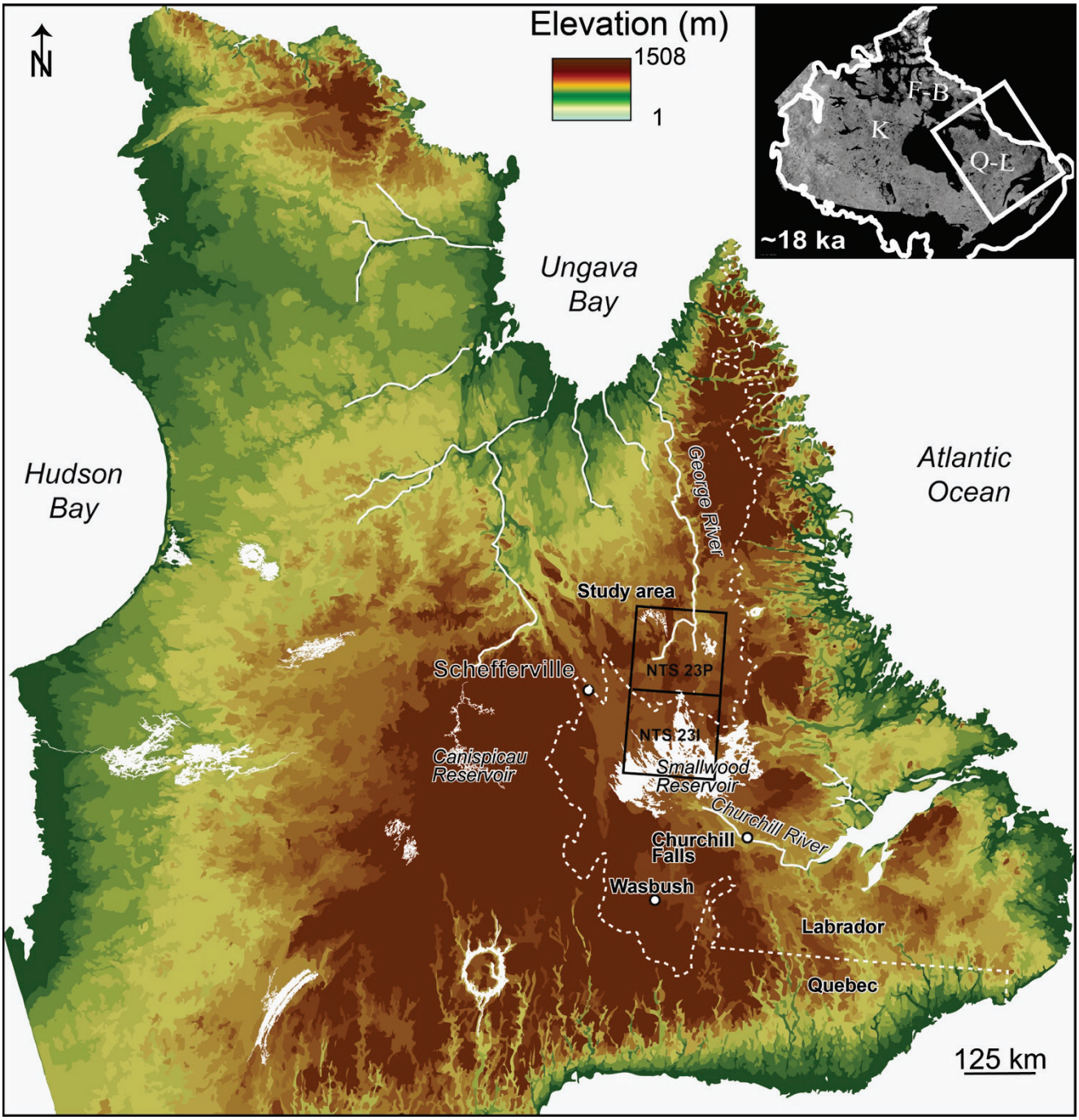

Figure 1. Location of the study area (black box), straddling the provincial border of Quebec and Newfoundland and Labrador (white dotted line). ***(Inset map)*** *The extent of the Laurentide Ice Sheet during LGM (~ 18 ka ^{14}C BP outlined by a thick white line showing major ice domes, the Keewatin (K) in the west, Foxe-Basin (F-B) in the north, and Quebec-Labrador (Q-L) in the east (from Dyke, 2004).*

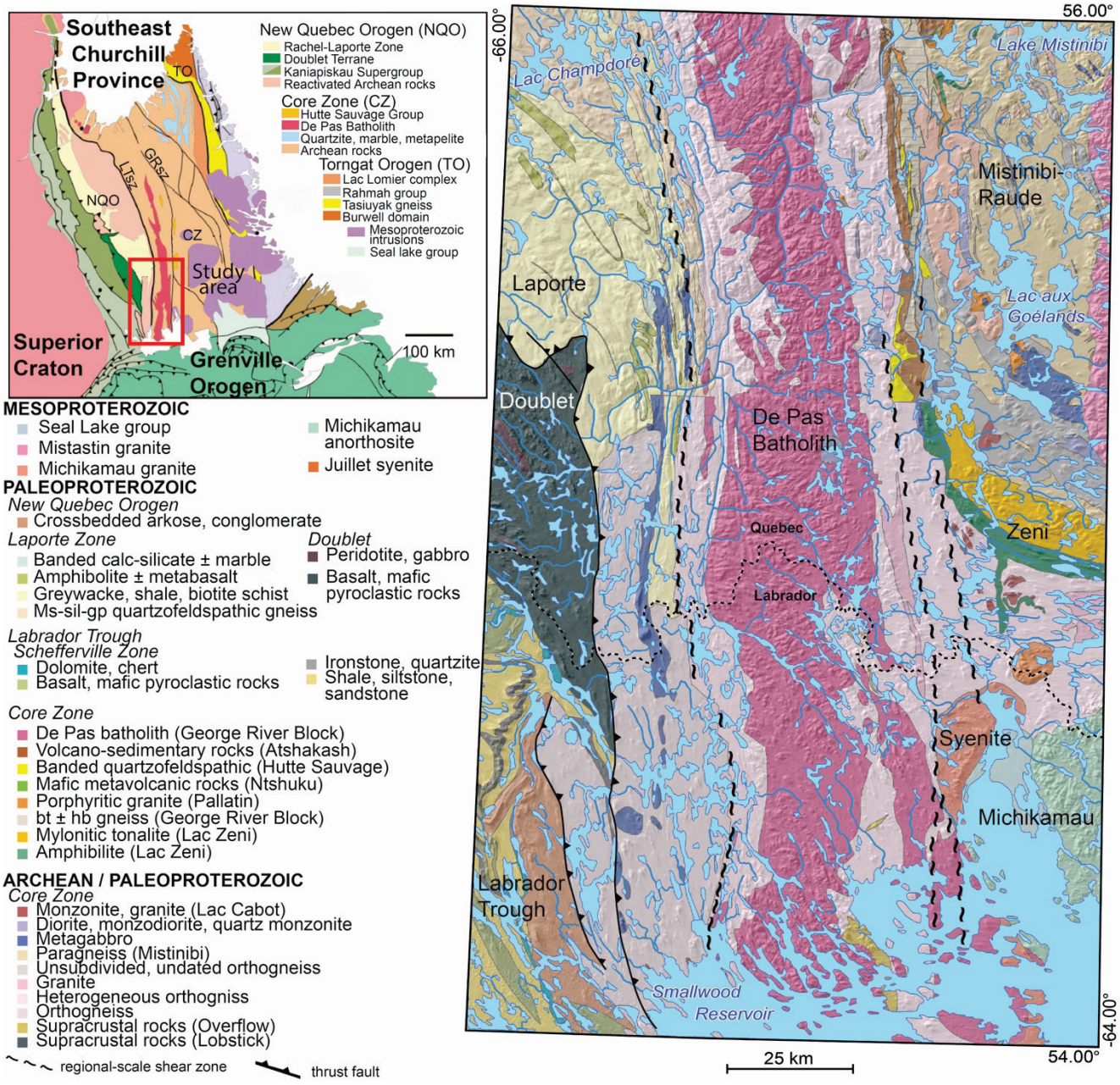

Figure 2. ***(Top Left):*** *simplified bedrock geology of the Core Zone within Quebec and Labrador (modified from James et al. 2003).* ***(Main Right)****: simplified bedrock geology of the study area (Wardle et al., 1997; Sanborn-Barrie, 2016; Corrigan et al., 2018). Major bedrock formations are indicated on the left.*

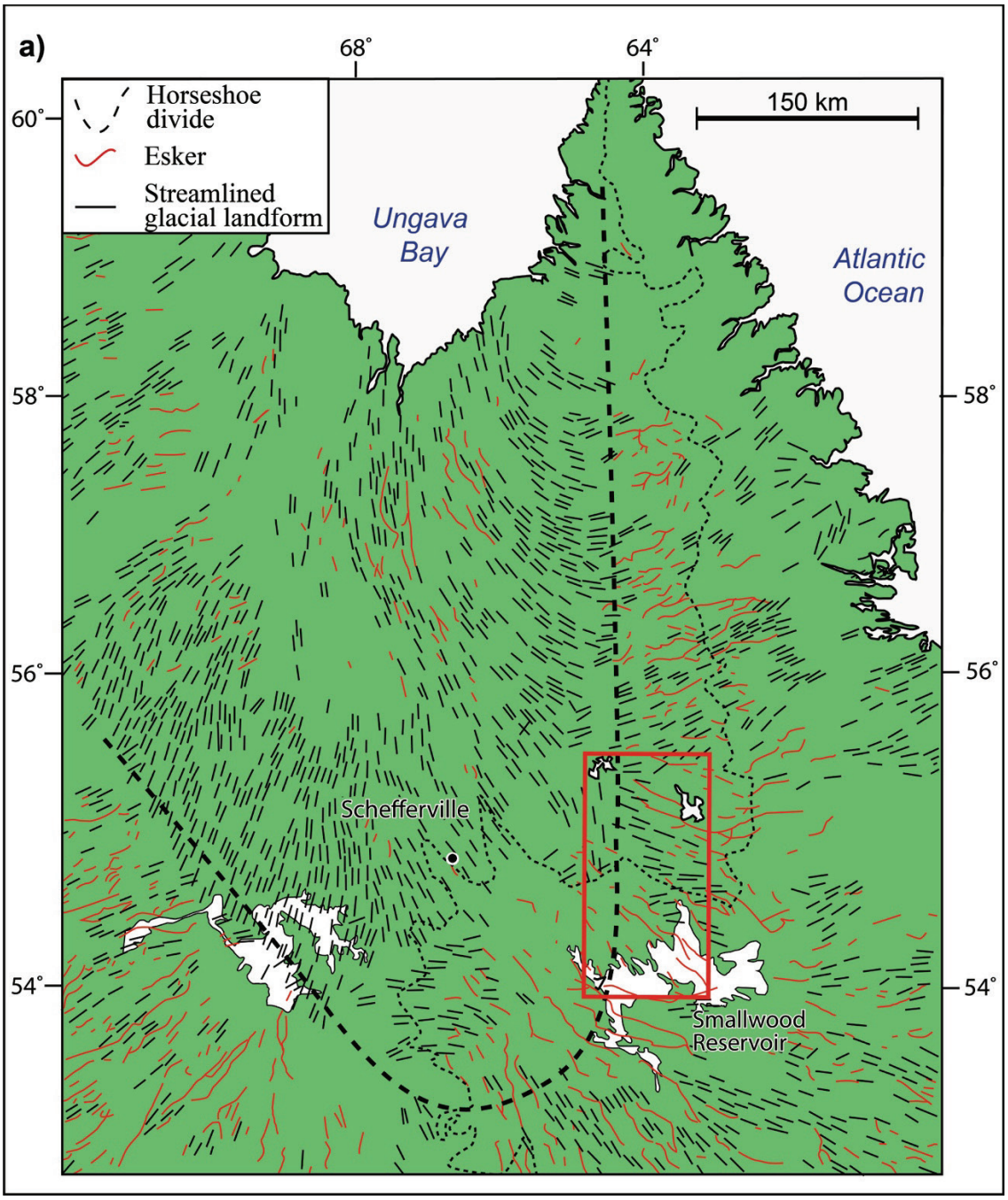
a)
68°
64°
60°
58°
56°
54°
Horseshoe divide
Esker
Streamlined glacial landform
150 km
Ungava Bay
Atlantic Ocean
Schefferville
Smallwood Reservoir

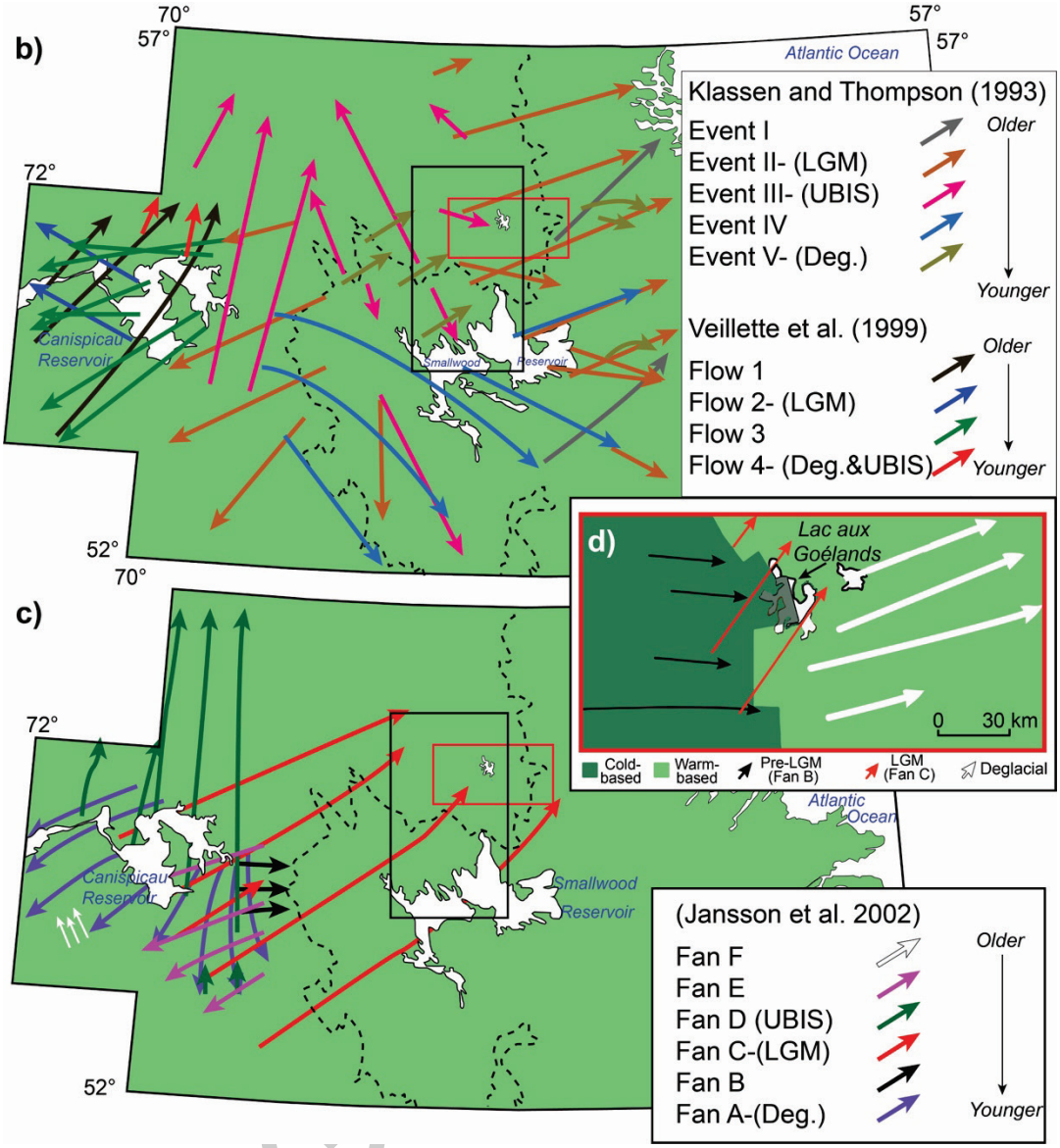

Figure 3 ***(a)*** *Map of east-central Quebec and western Labrador showing subglacial streamlined landforms and eskers with the U-shaped boundary as identified by Clark et al. (2000) indicated by the dashed line. This "horseshoe" unconformity separates converging landforms into Ungava Bay from landforms oriented in the opposite direction. The GEM-2 study area is indicated by the red box. Landforms are from Fulton (1995).* ***(b)*** *Ice-flow reconstructions of Klassen and Thompson (1993) and Veillette et al. (1999) for the surrounding region. Five and four ice flow phases were identified respectively; the GEM-2 study area is outlined in black, and Figure D outlined in red. UBIS is the Ungava Bay ice stream, LGM is Last Glacial Maximum, and Deg. are deglacial ice-flow phases.* ***(c)*** *Ice-flow reconstruction of Jansson et al. (2002).* ***(d)*** *Ice-flow reconstruction from fieldwork conducted south of Lac aux Goélands by Clarhäll and Jansson (2003) with their two earliest ice flows in opposing chronology to Klassen and Thompson (1993) and Veillette et al. (1999). Modified from Rice et al. (2019).*

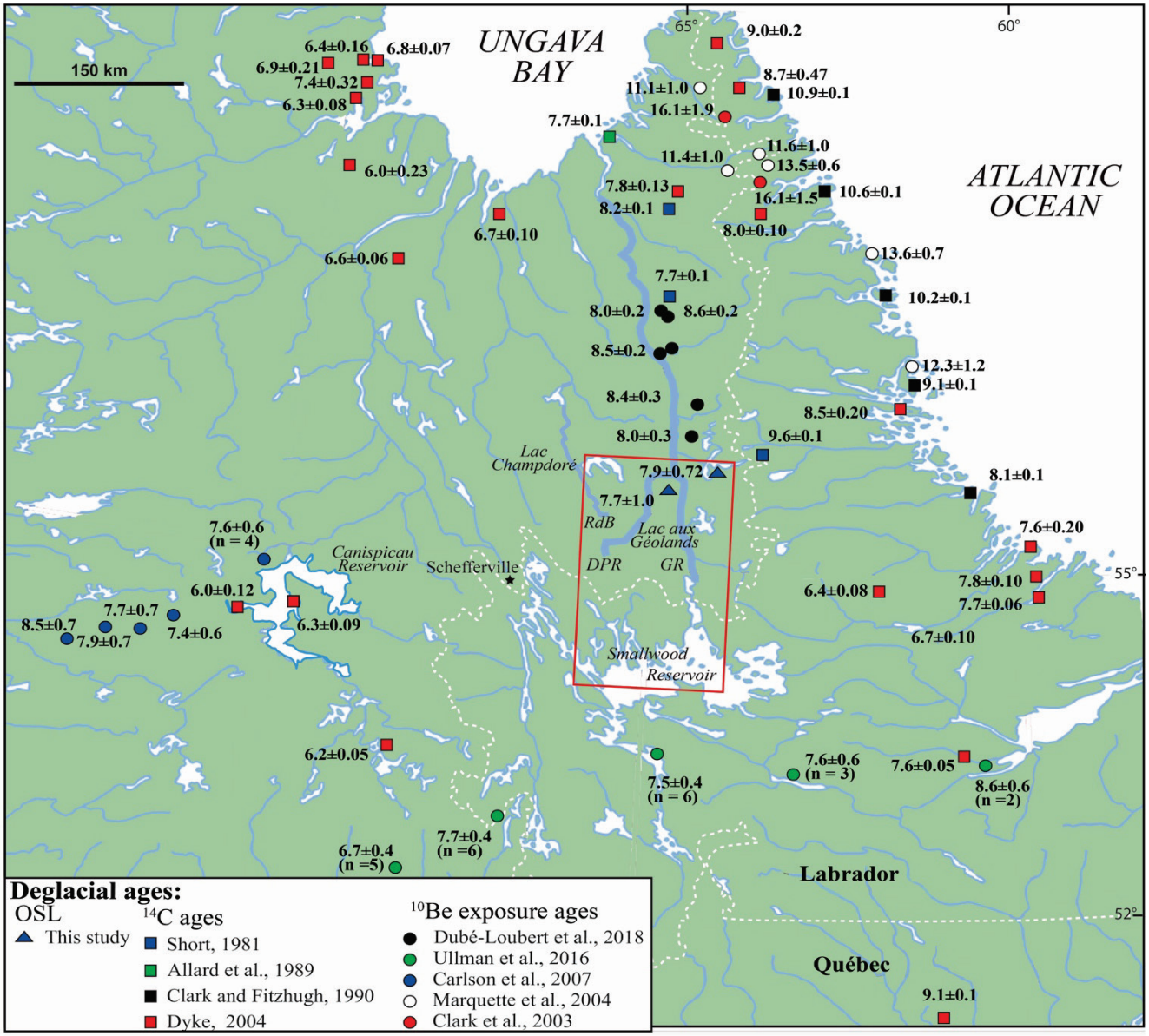

Figure 4. Location of the study area (red box) showing previously reported deglacial ages. Deglacial ages are reported in thousands of calibrated years before present (ka cal. BP). RdB indicates the Rivière à la Baleine, DPR indicates the De Pas River, and GR indicates the George River.

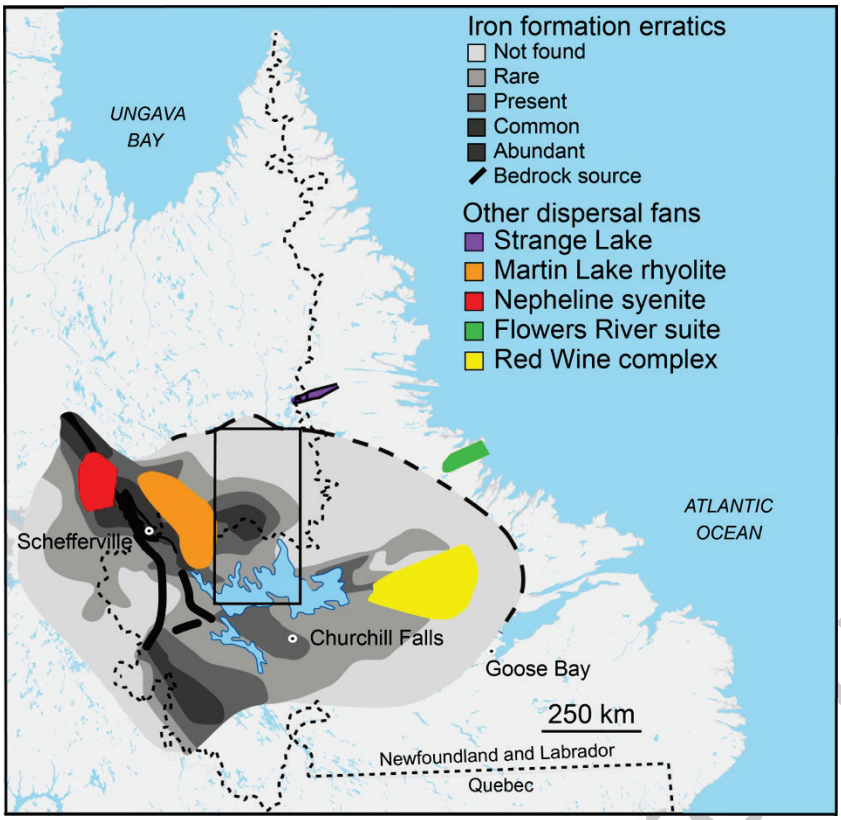

Figure 5. Dispersal patterns identified from erratic boulders by Klassen and Thompson (1993) for iron formation (greyscale) and other unique bedrock lithologies in western Labrador and east-central Quebec (modified from Klassen and Thompson, 1993). The study area is outlined in black.

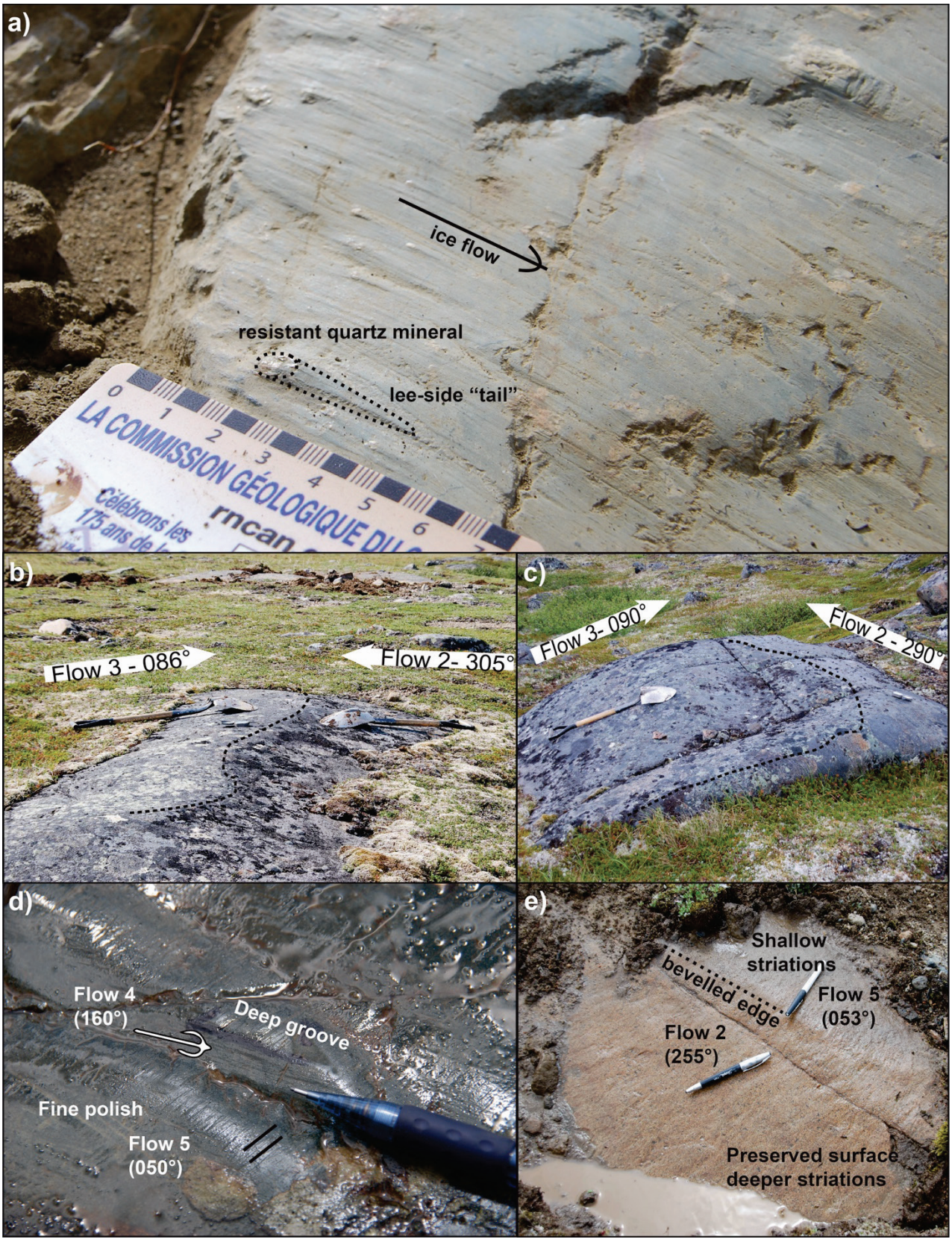

Figure 6. Examples of outcrop-scale ice-flow indicators: ***(a)*** *mini crag-and-tail;* ***(b)*** *and* ***(c)*** *double-stoss and lee outcrops formed during near complete ice-flow reversals;* ***(d)*** *fine polish (i.e., shallow striations) on outcrop indicative of late glacial ice-flow phase (Flow 5) with older deeper grooves parallel to pen tip (Flow 4);* ***(e)*** *lee-side preservation of older flow (Flow 2) from subsequent ice-flow phases (Flow 5), with a bevelled edge indicating the limit of preservation.*

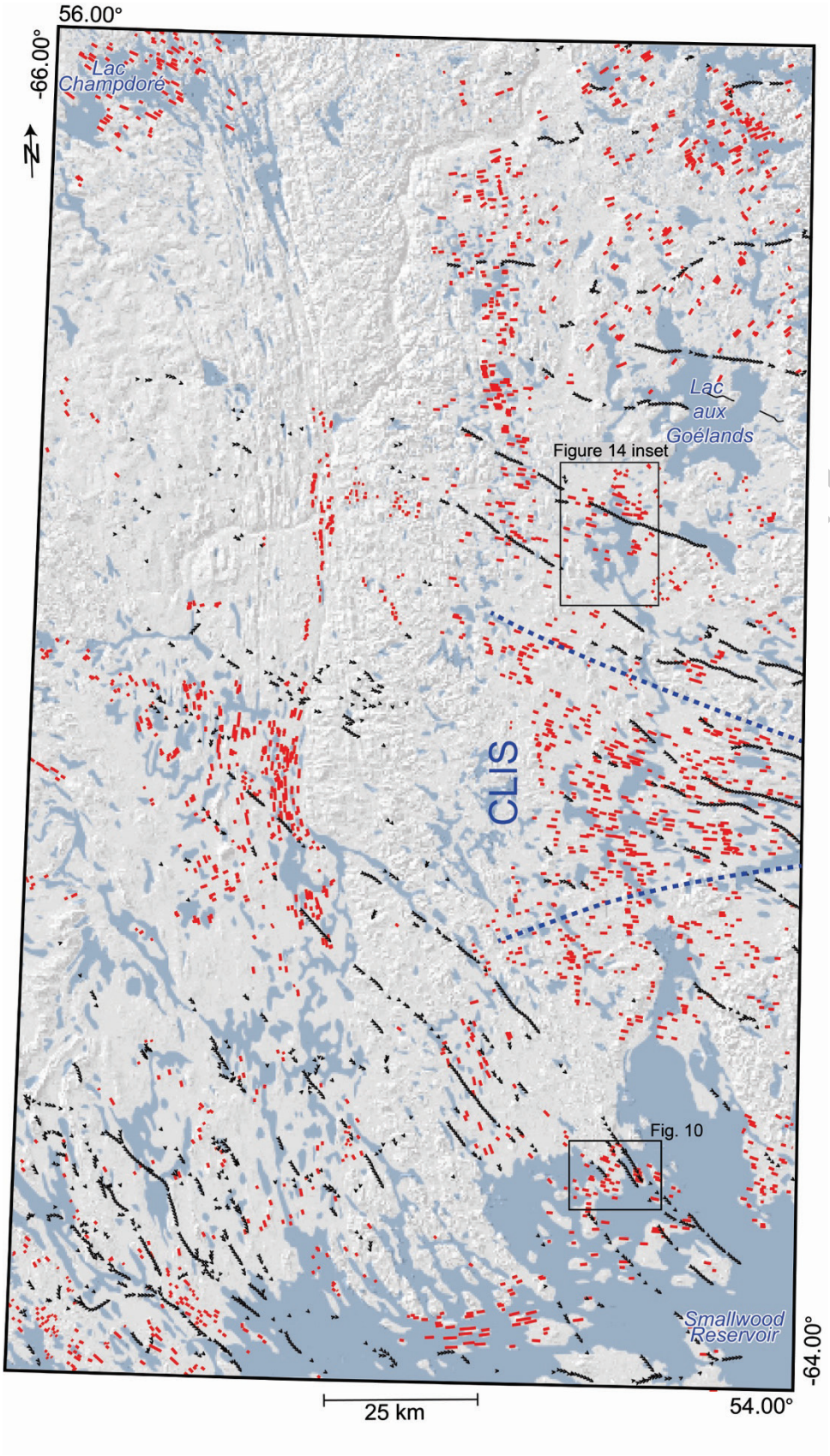

Figure 7. Distribution of elongated subglacial landforms (red lines) and eskers (black lines) across the study area. The Cabot Lake ice stream (CLIS) has been outlined with a blue dotted line (extracted from Rice et al., 2017c, d; Paulen et al., 2017, 2019a,b, 2020c, d; Cambell et al., 2018).

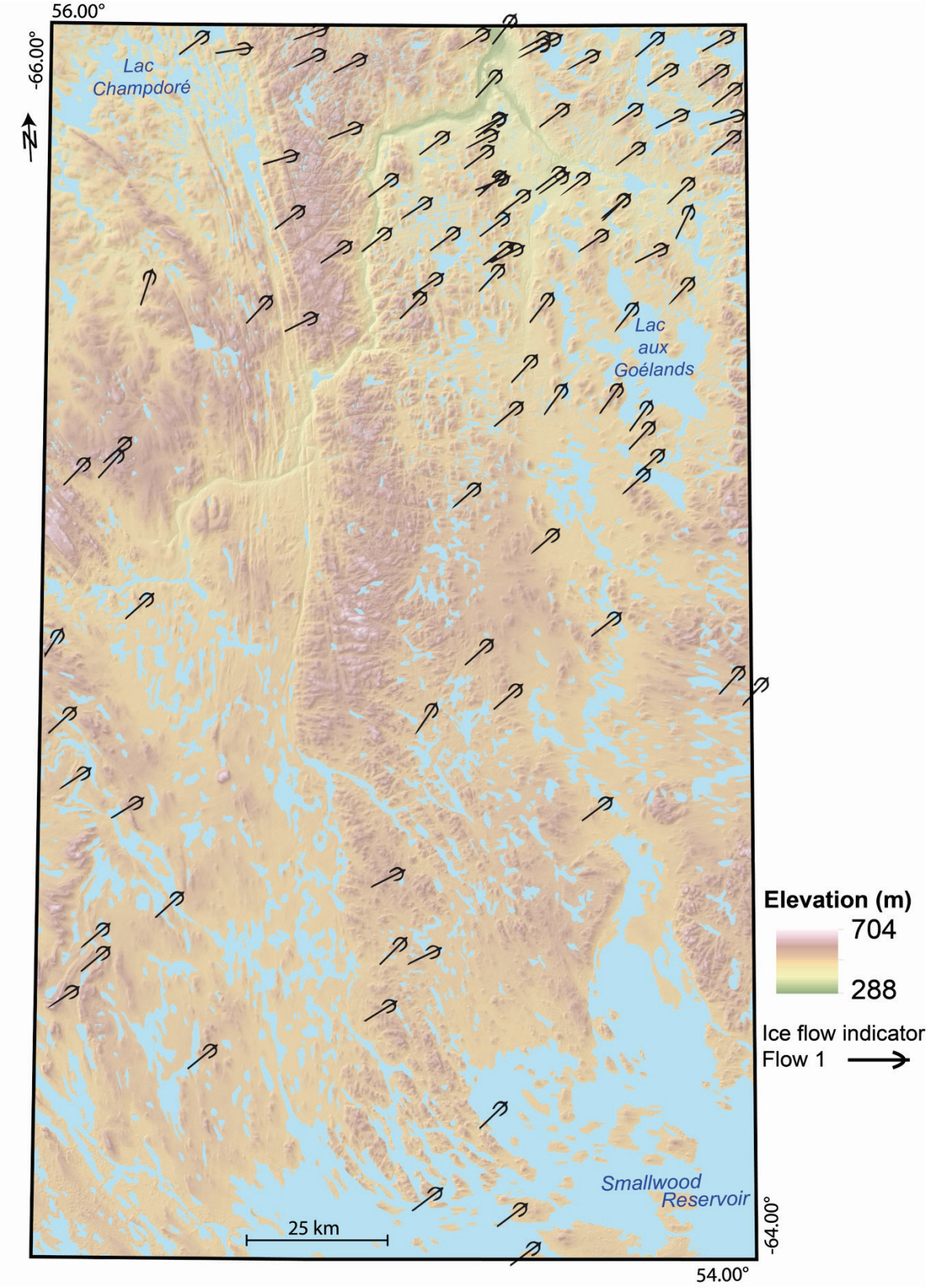

Figure 8. Outcrop-scale ice flow indicators associated with Flow 1, indicating a relatively uniform flow direction to the northeast across almost the entire study area. In the northeast corner of the map, Flow 3 striations are along a similar azimuth and are therefore difficult to differentiate from Flow 1 (see Rice et al. (2020d) and text for details).

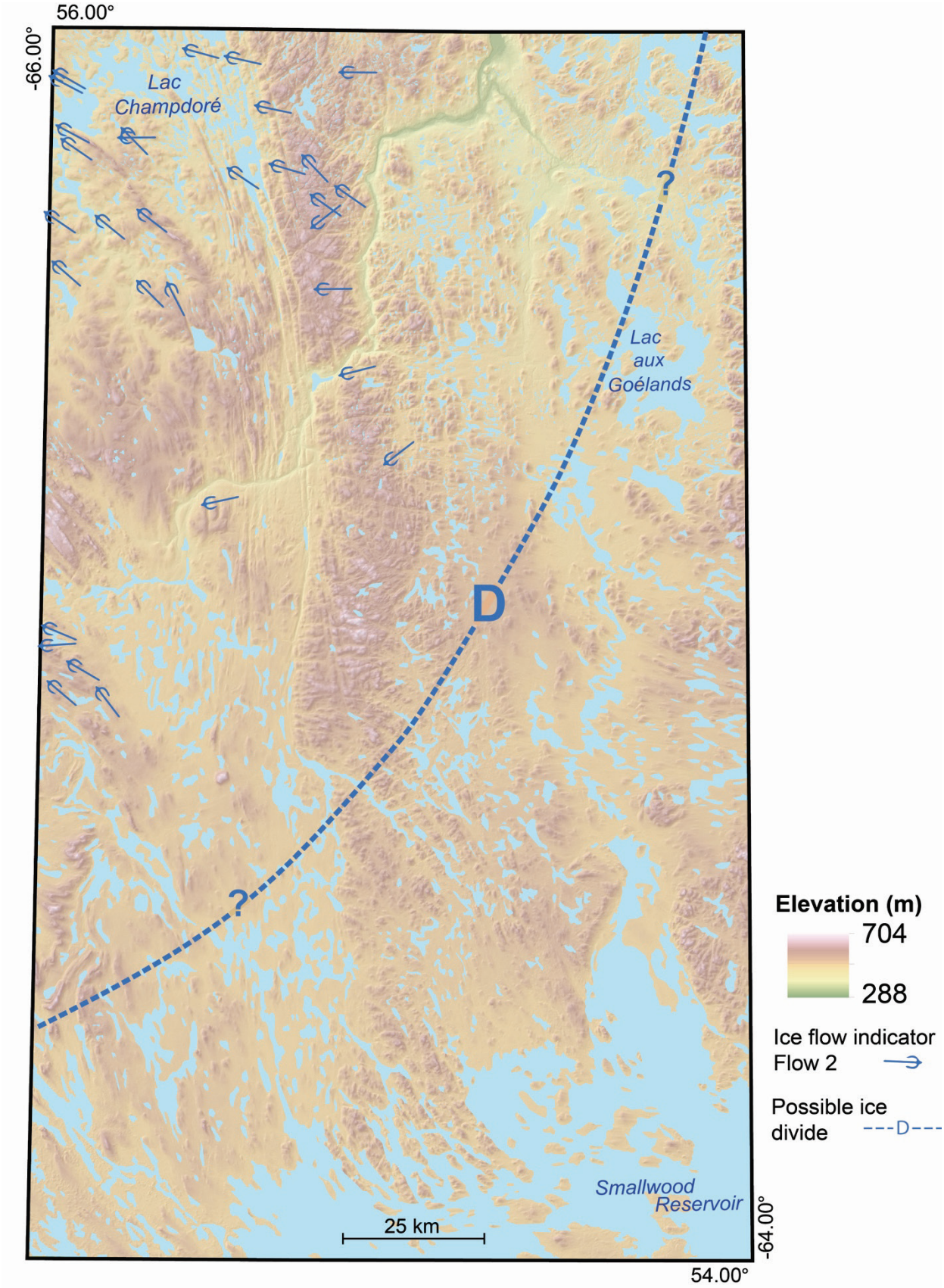

Figure 9. Outcrop-scale ice-flow indicators associated with Flow 2 are influenced in the northwest by a drawdown into Ungava Bay to the northwest. A local ice divide was located somewhere across the study area (approximate location indicated on map) to account for landforms related to Flow 2 and preservation of the Flow 1 record (see Fig. 10).

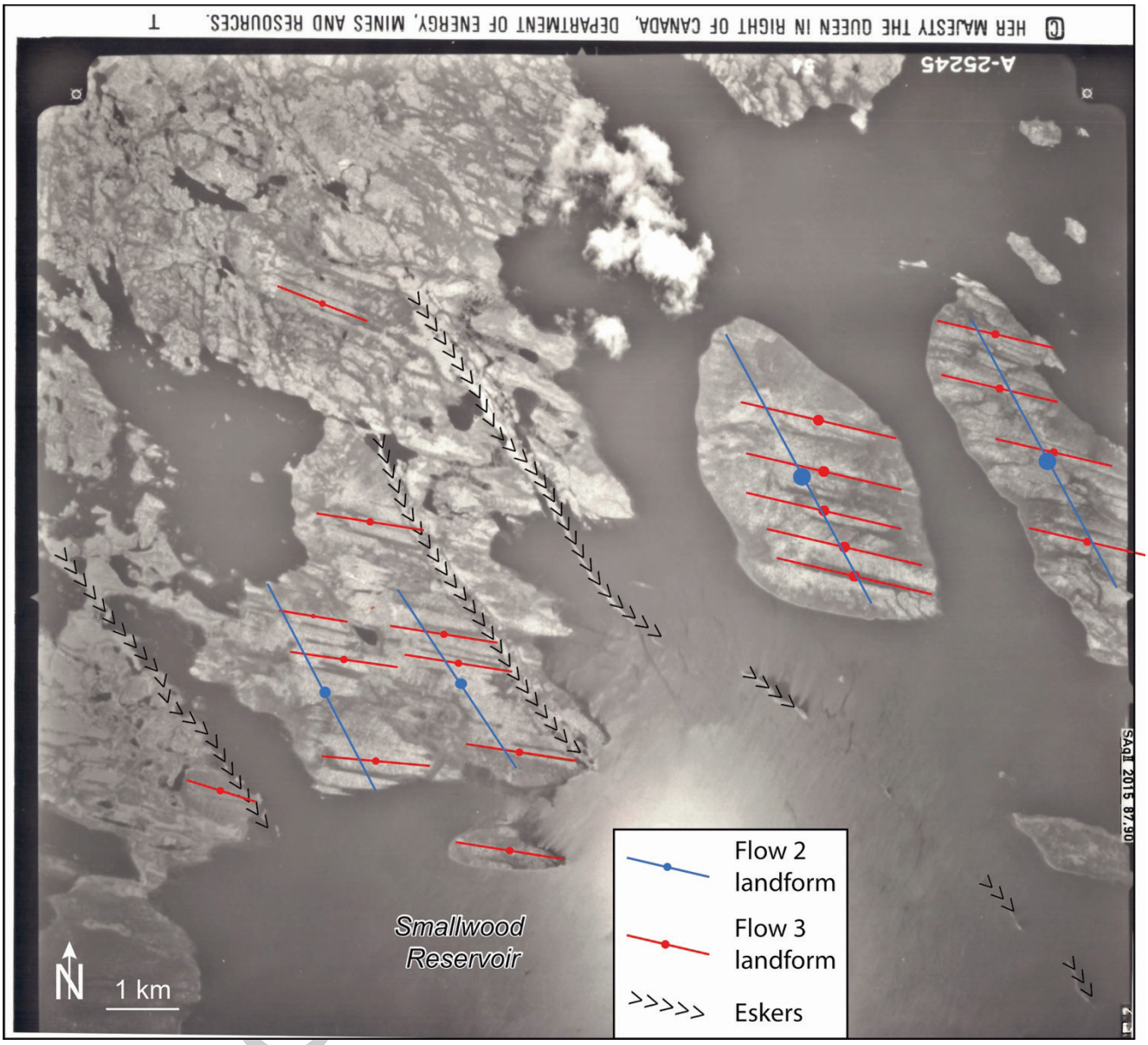

Figure 10. An example of palimpsest landforms in the Smallwood Reservoir, whereby southeast-trending landforms from Flow 2 (blue) are overprinted by smaller east-southeast-trending landforms during Flow 3 (red). Note that eskers crosscut the Flow 3 landforms and are closer in orientation to Flow 4 (see Figure 12; aerial photograph A25245-54, National Air Photo Library, Ottawa).

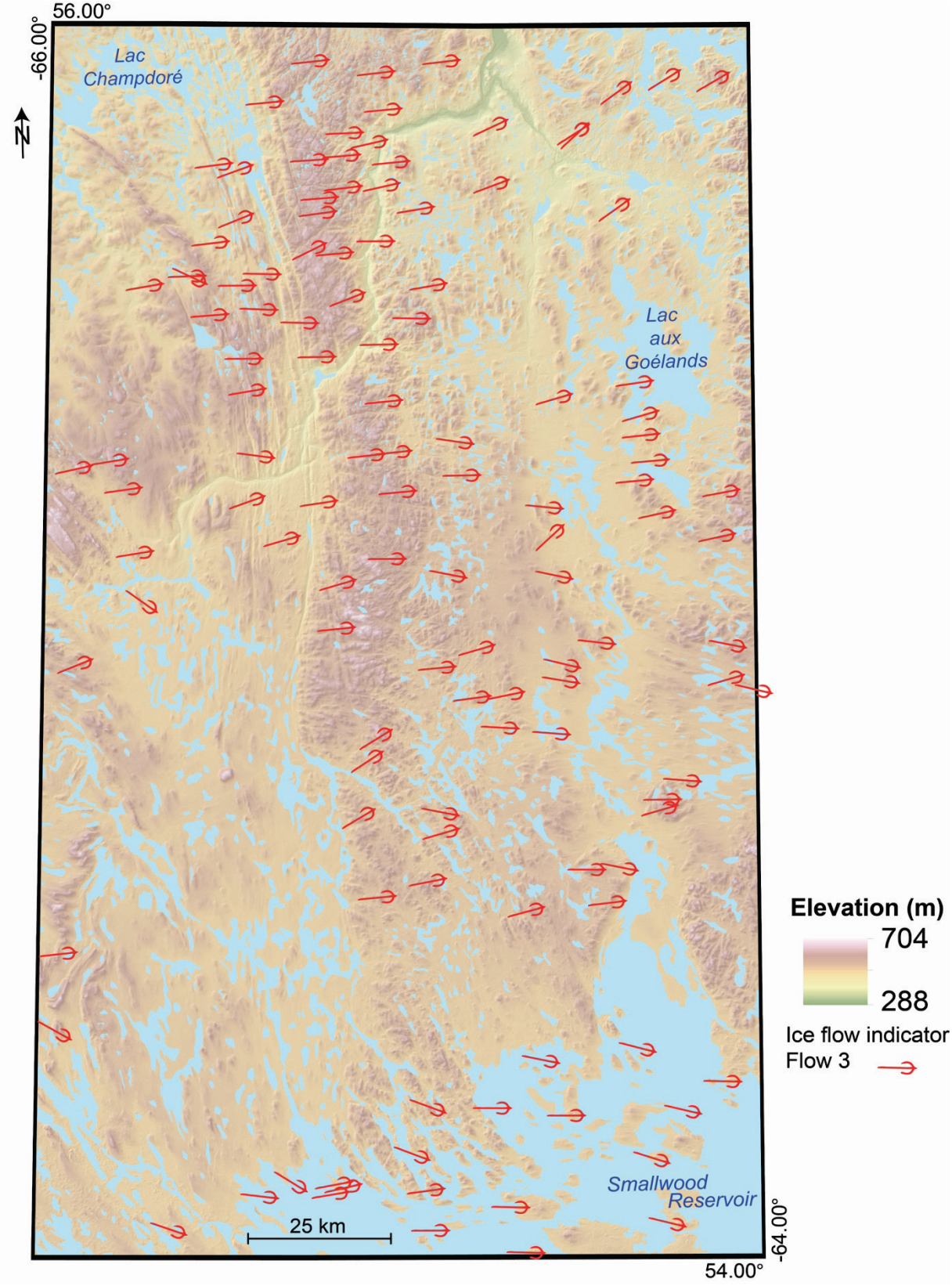

Figure 11. Outcrop-indicators associated with Flow 3 showing prevalent flow to the east, which followed the westward migration of the ice divide (then located outside of the study area). Small landforms associated with Flow 3 were identified in the northeast of the study area (Rice et al., 2020c), however, the striation record is difficult to discern from Flow 1 where crosscutting relationships are not evident (see Figure 8). Where no cross-cutting relationship could be established, the striation were assigned to Flow 1.

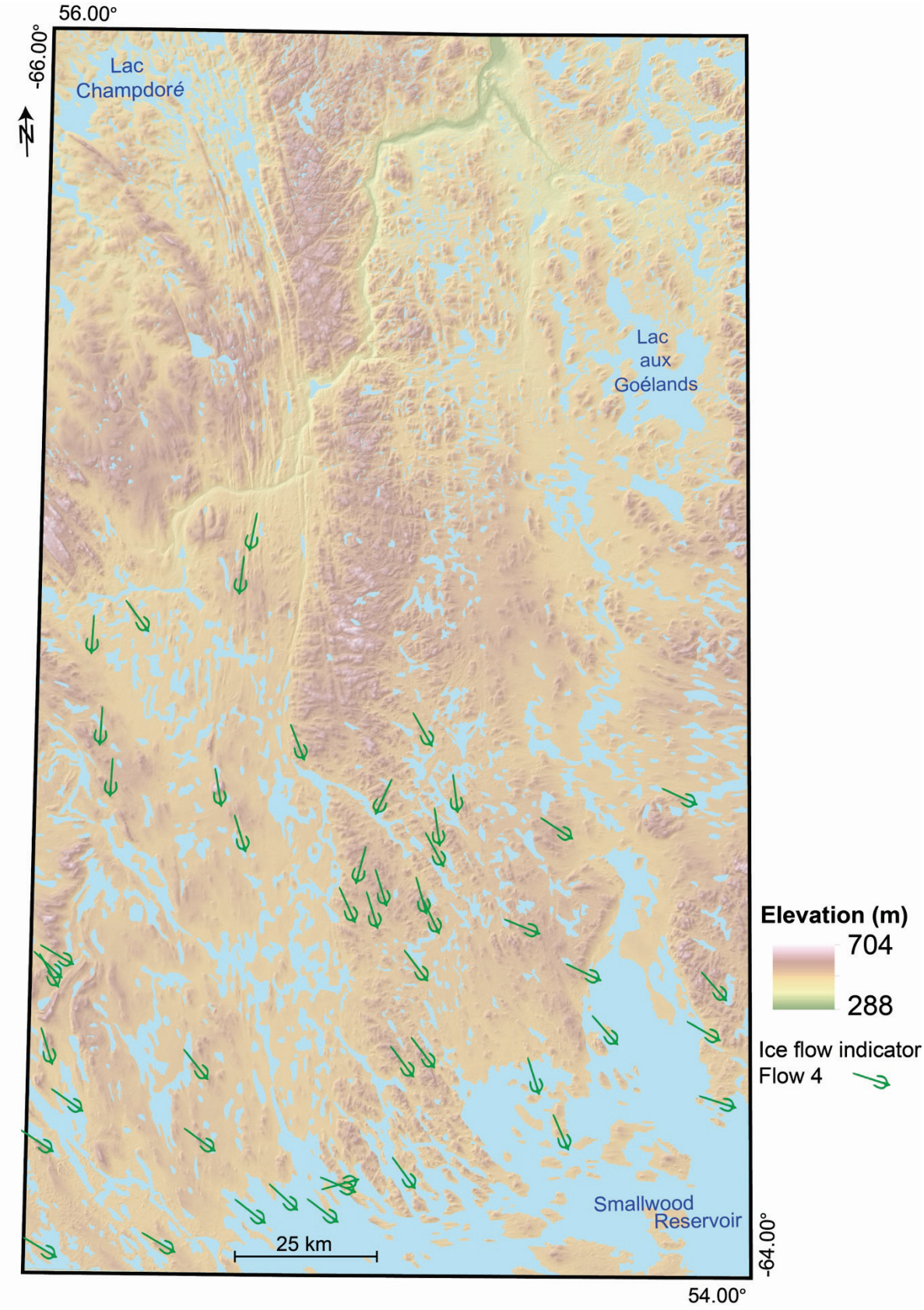

Figure 12. Outcrop-scale ice-flow indicators associated with Flow 4. Following the westward migration of the ice divide, ice was deflected south by the topographic highlands in the middle of the study area (De Pas Batholithi in Figure 2) and continued to flow southeast into the Smallwood Reservoir.

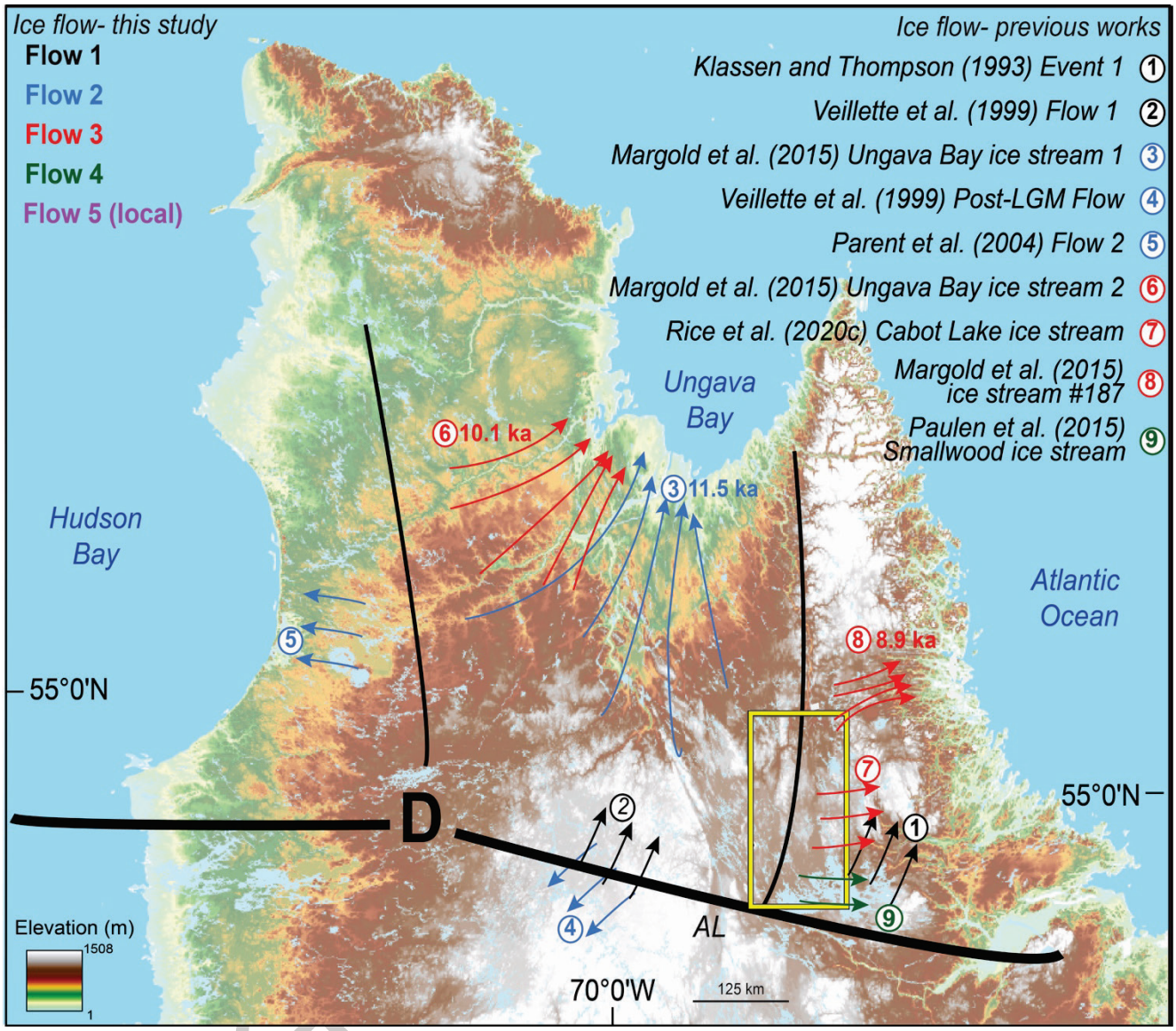

Figure 13. Regional ice-flow phases across Quebec and Labrador with each ice-flow phase correlated to the ice-flow reconstruction from this study (study area outlined in yellow; Flows 1 to 5 in the top left corner). Assigned ages to ice flow events by Margold et al. (2018) have been indicated next to the identifying number (ages are reported in cal ka BP). Note Flow 5 is a localized flow and not recorded at the regional scale and therefore is not associated to any ice streaming events. D represents the centre of the Quebec-Labrador dome and the thick black lines represent major ice divide locations, with the AL identifying the Ancestral Labrador Ice Divide, and the thinner lines represent ice saddles (Dyke and Prest, 1987).

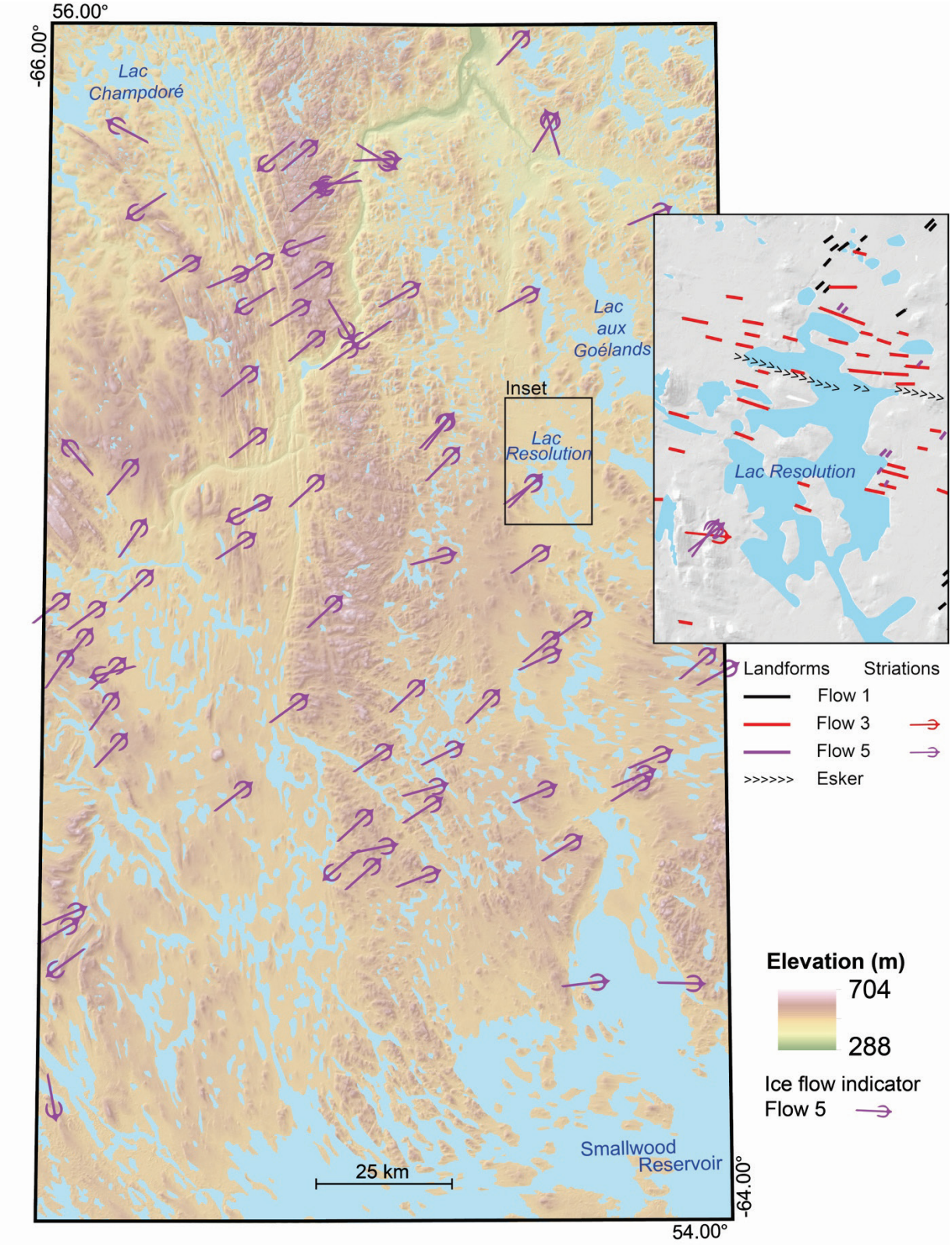

Figure 14. Outcrop-scale ice-flow indicators associated with Flow 5, when the ice sheet had thinned enough that local topography became a major factor in controlling local ice-flow directions. As the ice sheet thinned, it split into multiple different smaller ice caps and in some regions reworked existing landforms. ***Inset:*** *Landforms and striations showing Flow 1 landforms (black lines) reworked by Flow 3 (red lines) in the top of the inset and therefore must have formed prior to Flow 3 and are not related to Flow 5. Conversely, Flow 3 landforms are reworked by Flow 5 (purple lines) in the centre of the inset indicating Flow 5 reworked the Flow 3 landforms and were not formed during Flow 1. Striations recorded on a local upland show the relative chronology between Flow 3 and Flow 5.*

Figure 15. Geochronological results from the study area underlain by surficial geology maps (from Rice et al., 2017a, b; Paulen et al., 2017, 2019a,b, 2020, 2022; Campbell et al., 2018). White dots represent results from bedrock and erratic (E) samples analyzed for cosmogenic ^{10}Be. Yellow dots represent optically stimulated luminescence age on beach sands. Several anomalous ages are considered outliers and are not interpreted to reflect deglacial timing (see text).

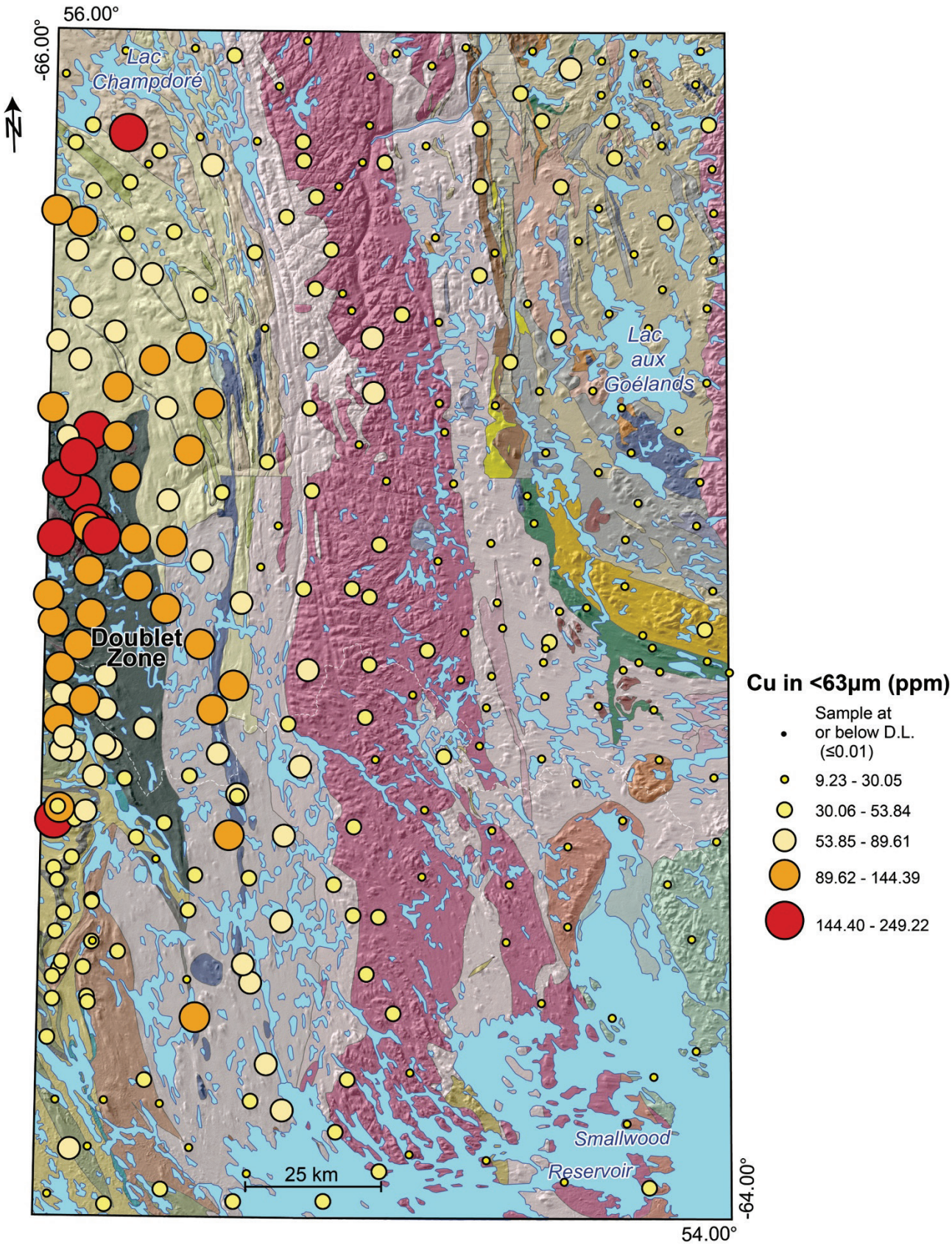

Figure 16. Proportional dot map of Cu concentrations in the <63 µm fraction of till samples analyzed by aqua regia/ICPMS (see Figure 2 for bedrock geology legend). The main source area of Cu lies within the Doublet Zone.

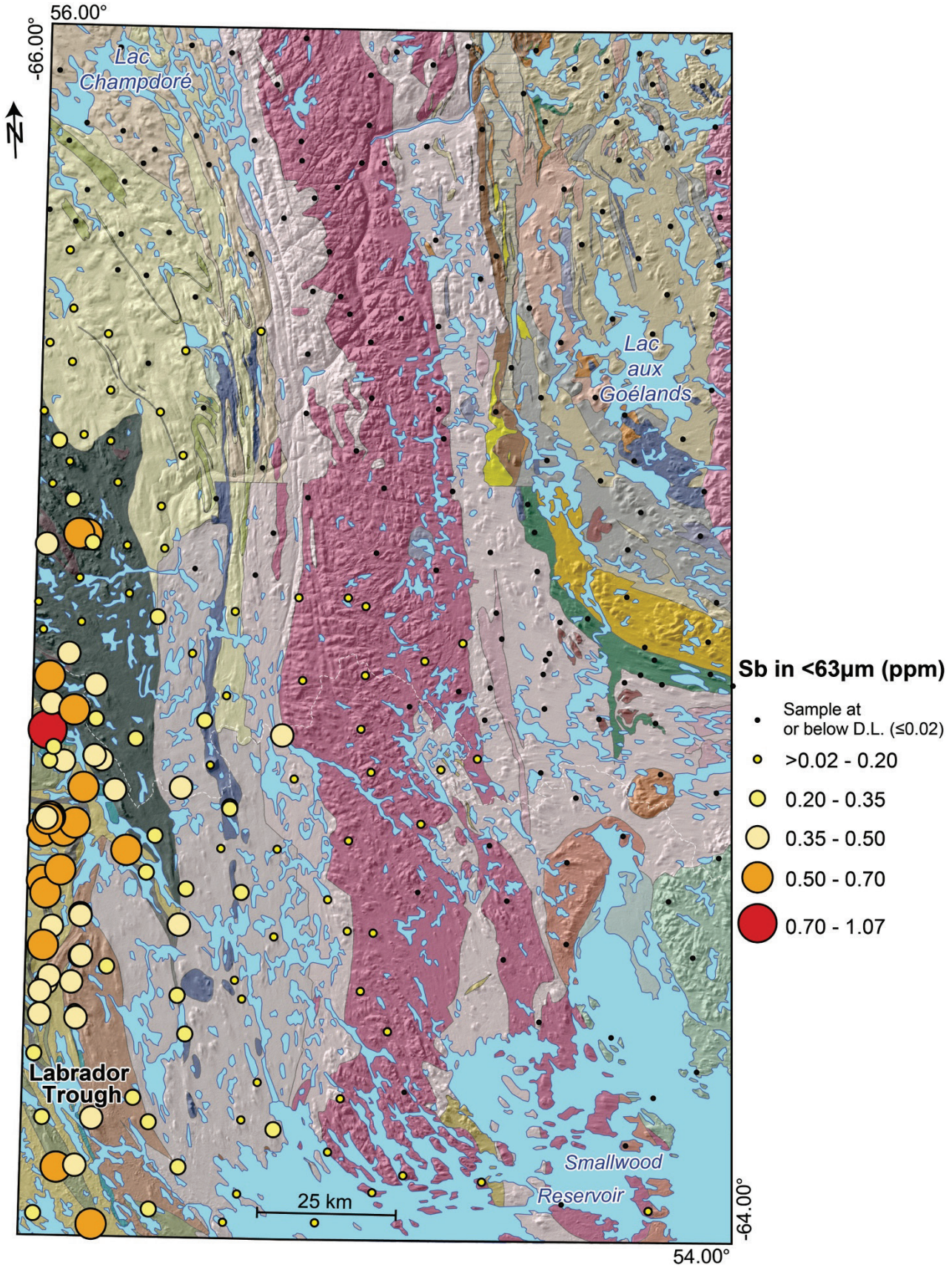

Figure 17. Proportional dot map of Sb concentrations in the <63 µm fraction of till samples analyzed by aqua regia/ICPMS (see Figure 2 for bedrock geology legend). The source area for Sb is the iron formations of the Labrador Trough.

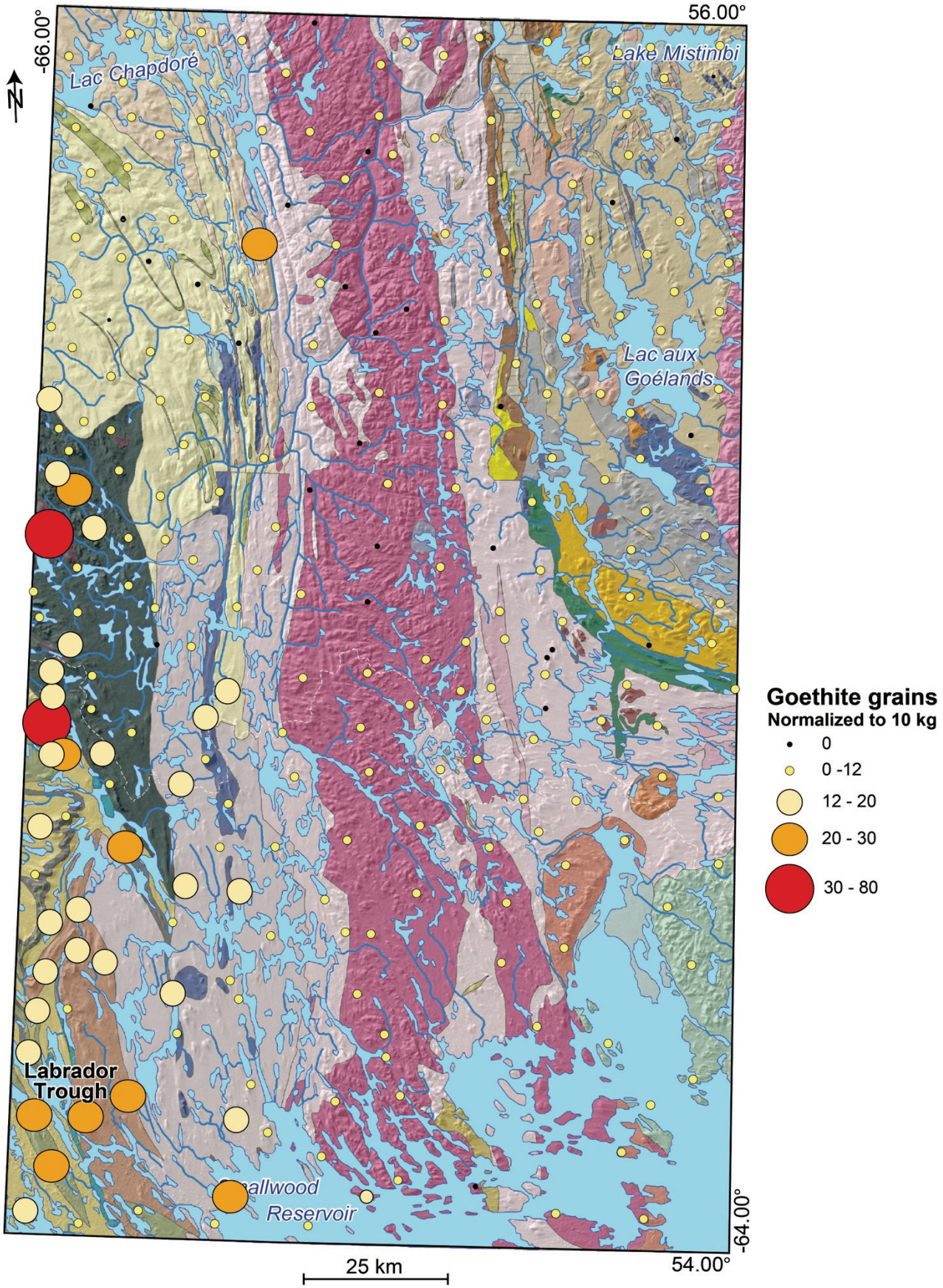

Figure 18. Proportional dot map of goethite grains abundance (normalized to 10 kg) in the 0.25 – 0.5 mm fraction of till samples (see Figure 2 for bedrock geology legend). The source area for the goethite grains is in iron formations of the Labrador Trough.

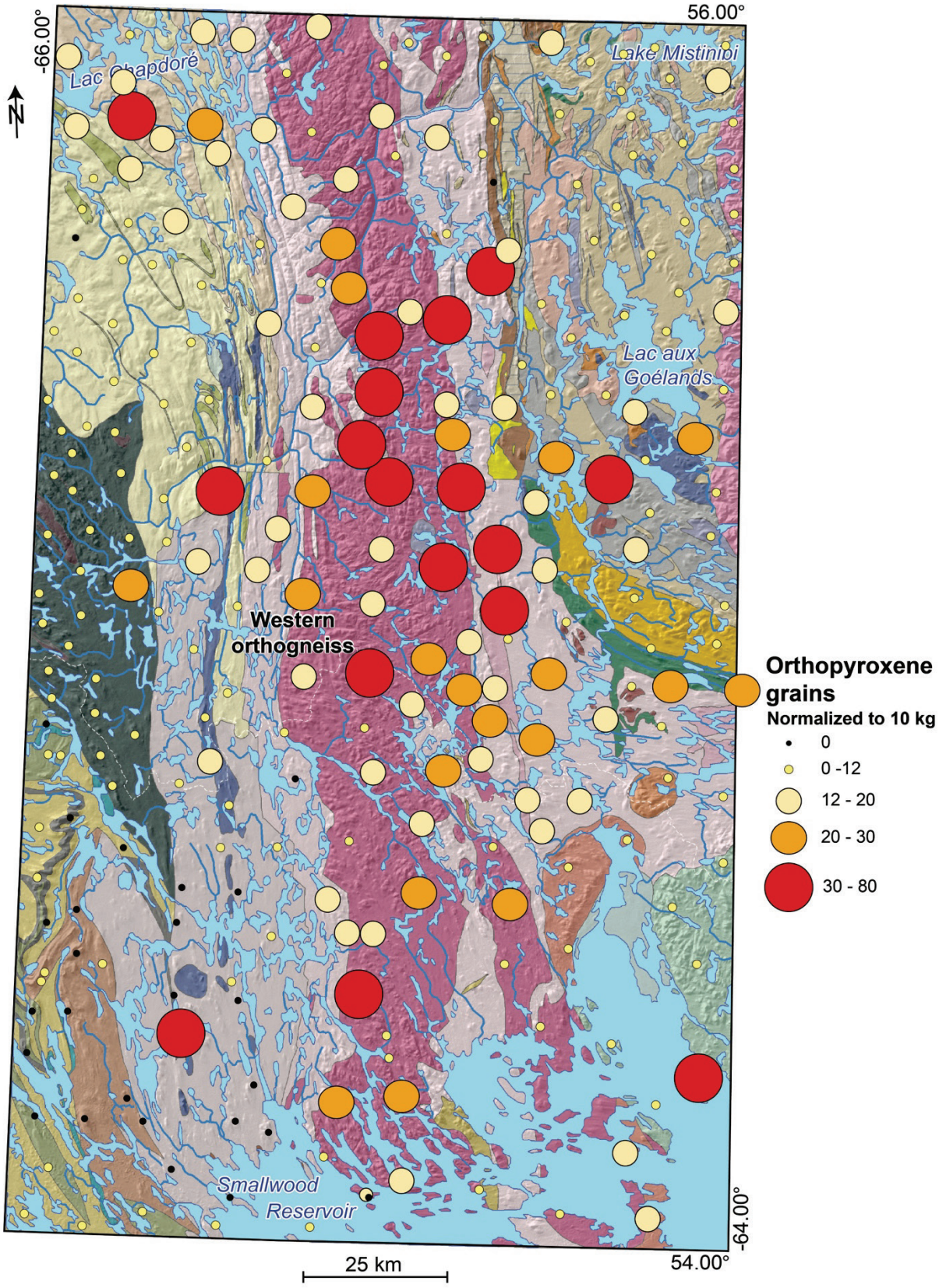

Figure 19. Proportional dot map of orthopyroxene grains abundance (normalized to 10 kg) in the 0.25 – 0.5 mm non-ferromagnetic fraction of till samples (see Figure 2 for bedrock geology legend). The source area for the orthopyroxene grains lies within the western orthogneiss.

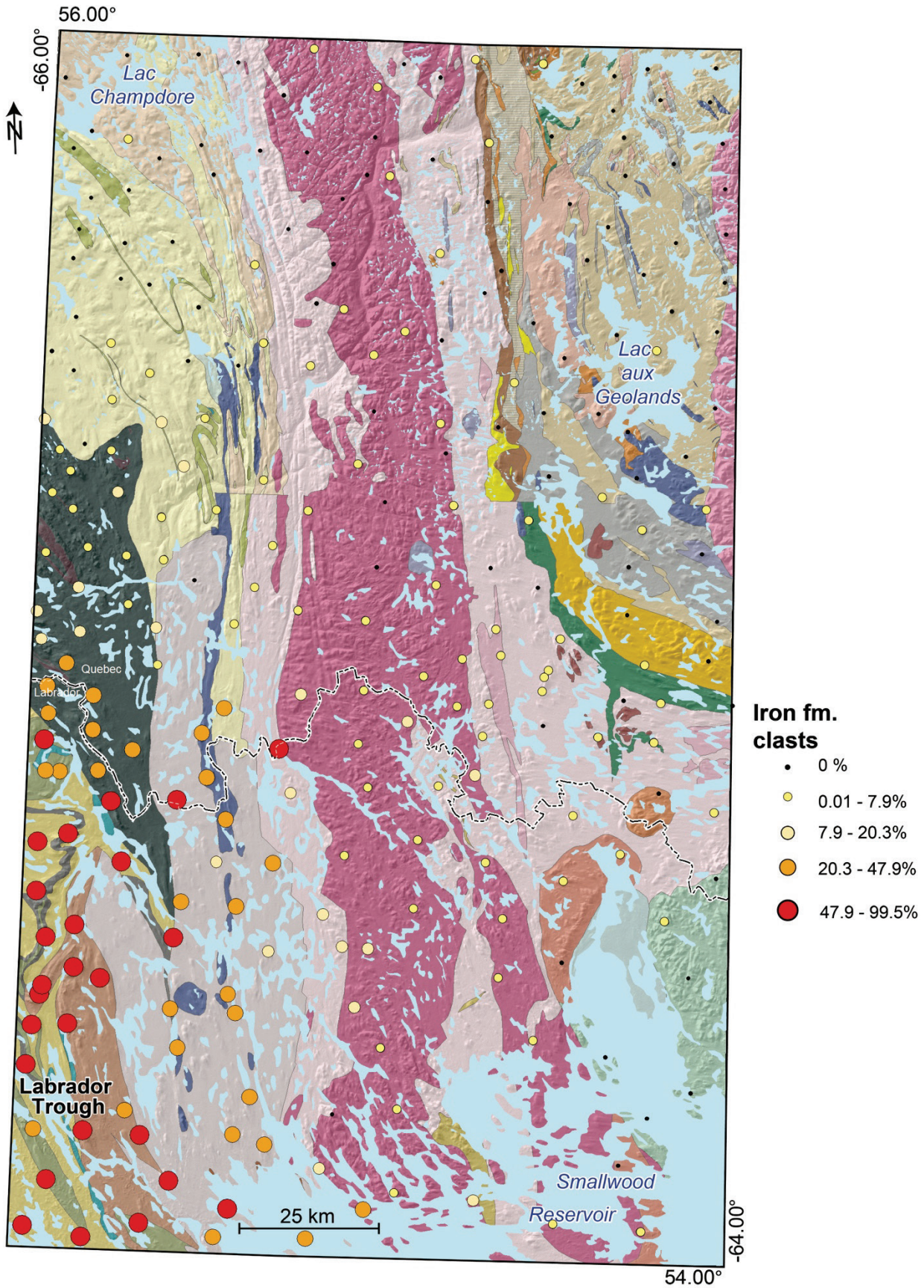

Figure 20. Proportional dot map of iron formation clasts in the 2 to 50 mm fraction of bulk till samples. Iron formation clasts were derived from the Labrador Trough (see Figure 2 for bedrock geology legend).

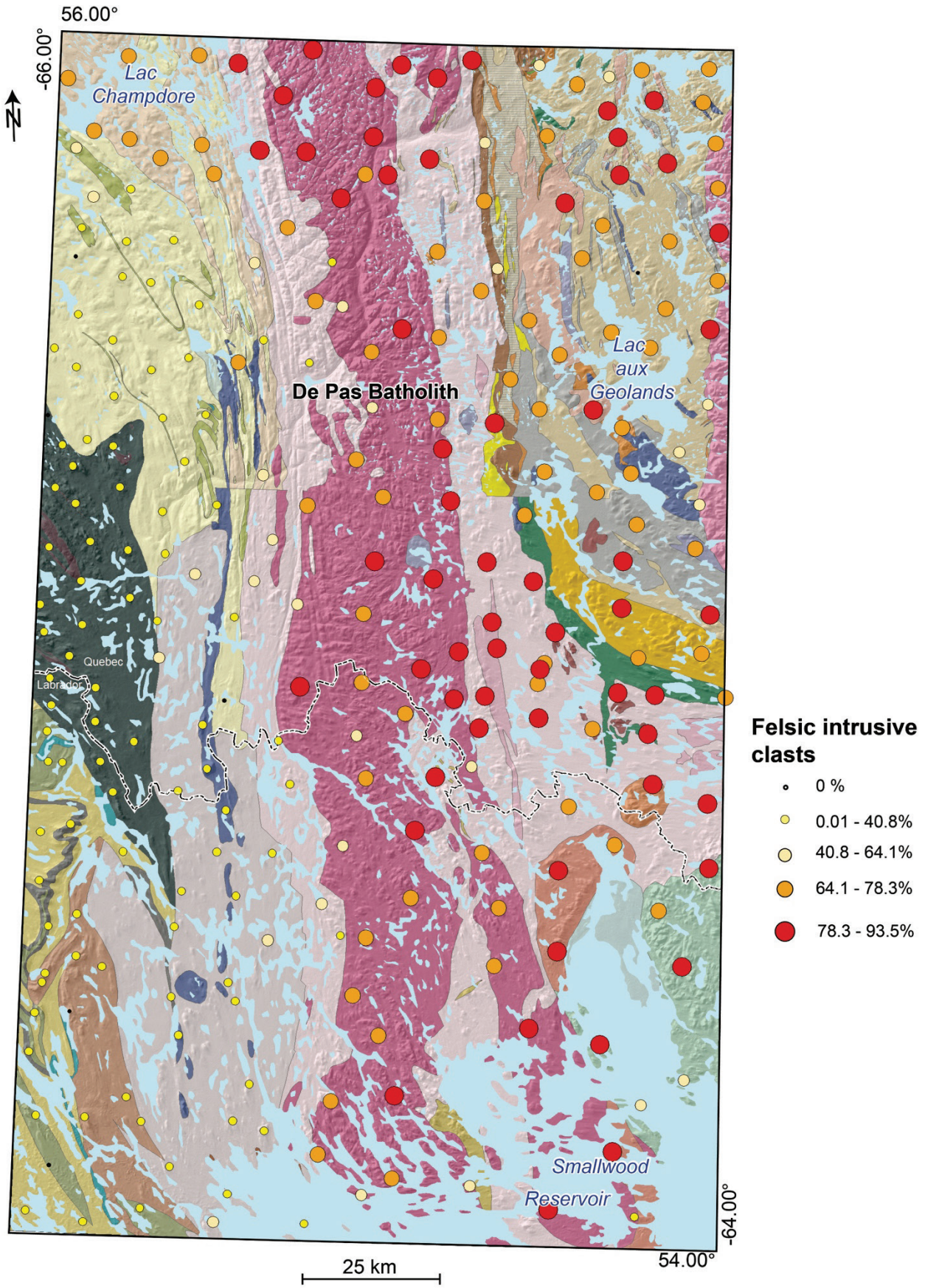

Figure 21. Proportional dot map of felsic intrusive clasts in the 2 to 50 mm fraction of bulk till samples. Felsic intrusive clasts were derived from the De Pas Batholith (see Figure 2 for bedrock geology legend).

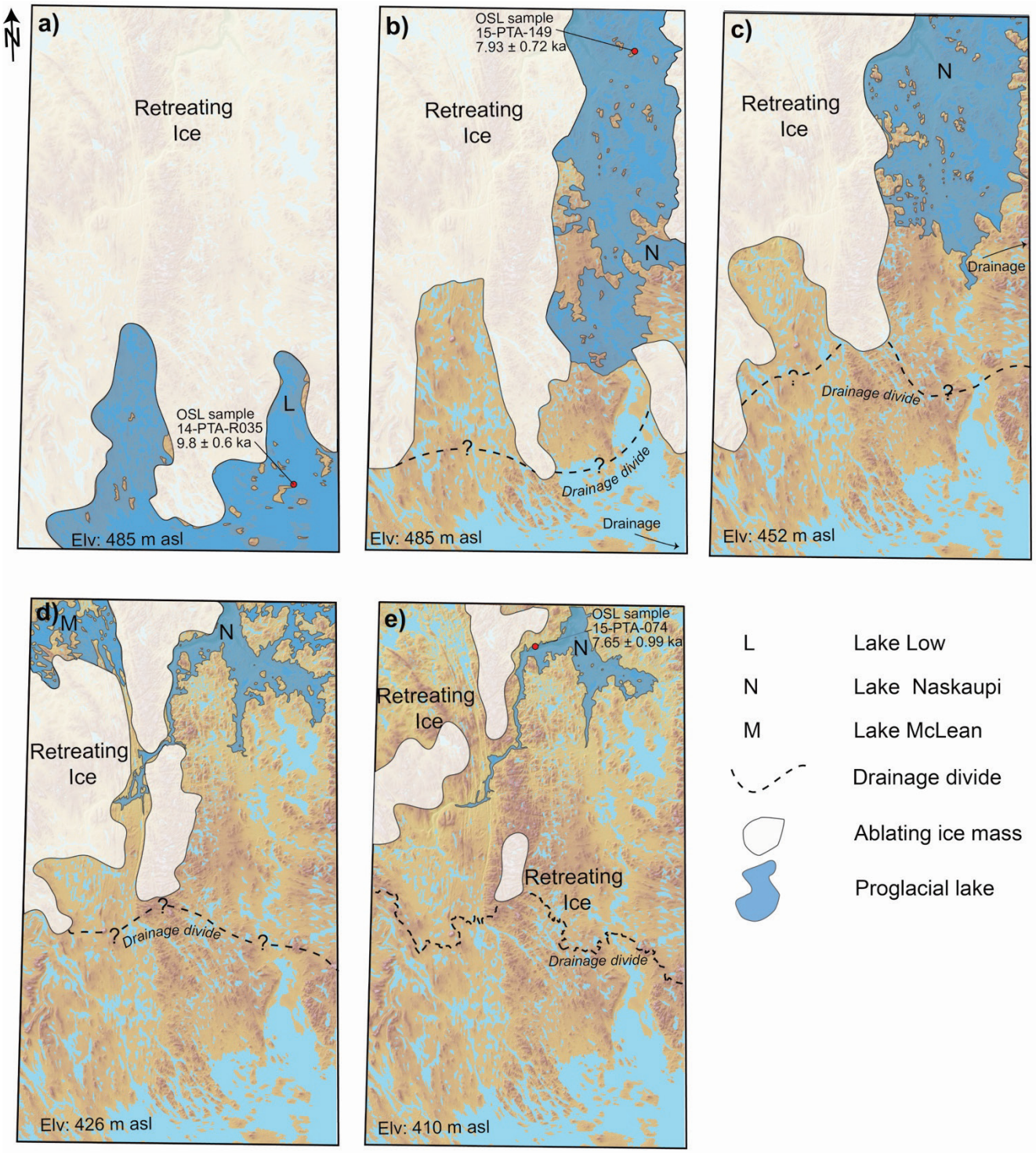

Figure 22. Paleogeographic reconstruction of the three glacial lakes within the study area, constrained by ice-margin retreat, DEM data, and OSL ages from beach sediments and terraced outwash sediments. The elevation of the lake is indicated in the bottom left of each relative lake stage.

Tables

Table 1. ^{10}Be sample information for bedrock and erratic (E) samples.

Sample	Lat. (°N)	Long. (°W)	Elev. (masl)	Corr. Elev. (masl)[a]	Thick (cm)	Topo. shielding correction	^{10}Be atoms/g	± atoms /g	Thickness scaling factor	Exposure age (yr)[b] ± error[c]
East										
15-PTA-058	55.843	-64.207	494	433	3.0	1	4.84E+04	1.23E+03	0.9756	7800 ± 200
15-PTA-078	55.821	-64.515	517	456	2.5	1	6.28E+04	1.24E+03	0.9796	9800 ± 200
15-PTA-081*	55.810	-64.189	559	498	2.0	1	6.10E+04	2.03E+04	0.9839	9200 ± 3100
15-PTA-081E*	55.810	-64.189	559	498	1.5	1	4.13E+04	1.37E+04	0.9879	6200 ± 2170
Centre										
15-PTA-077*	55.810	-65.080	495	434	3.0	1	4.35E+04	1.78E+04	0.976	7100±2900[d]
15-PTA-077E	55.810	-65.080	495	434	2.0	1	1.03E+05	2.35E+04	0.9839	16700 ± 3800[d]
16-PTA-070	55.784	-65.251	623	562	1.0	1	1.67E+05	3.14E+03	0.9918	24000 ± 500
West										
16-PTA-053	55.867	-65.709	517	456	3.0	1	5.36E+04	1.19E+03	0.9756	8500 ± 200
15-PTA083	55.772	-65.721	509	448	1.0	1	5.95E+04	1.14E+03	0.9918	9500 ± 200
15-PTA-021*	55.838	-65.729	529	468	2.0	1	5.07E+04	1.14E+04	0.9839	7900 ± 1800
South										
16-PTA-114B	54.181	-65.29	565	504	3.5	1	1.06E+05	1.79E+03	0.9756	16454 ± 300[d]

[a] Elevation were corrected to isostatic uplift by averaging the uplift from modern elevation using data from ICE-6G(VM5a) (Argus et al. 2014; Peltier et al. 2015)

[b] Be ages reported at 1-sigma AMS uncertainties and calculated using the scaling scheme for spallation of Lal (1991) and Stone (2000)

[c] error is reported to 1σ of internal uncertainty. Values have been rounded to nearest 10s value.

[d]Outlier samples

*Sample analyzed by PRIME lab.

Table 2. Optically stimulated luminescence (OSL) sample collection data.

Sample ID	Elev. (± 5 m.a.s.l)	Depth (cm)	H_2O[1] (Δ^w)	K (%)	Rb (ppm)	Th (ppm)	U (ppm)	D_e (CAM) (Gy)	Uncorrected CAM age (ka)	Fading-corrected CAM[2] age estimate (ka)[3]	Fading-corrected MAM[2] age estimate (ka)[3]
15-PTA-035	464	100	0.0088 ± 0.001	2.50 ± 0.13	52.5 ± 2.77	3.00 ± 2.77	0.39 ± 0.08	23.0 ± 4.0	40.0 ± 3.2	61.9 ± 5.02	29.9 ± 3.10
15-PTA-074	314	370	0.185 ± 0.002	1.80 ± 0.1	61.8 ± 3.31	5.50 ± 0.28	2.13 ± 1.69	7.0 ± 1.0	6.13 ± 0.79	7.65 ± 0.99	n/a
15-PTA-149	486	75	0.0329 ± 0.003	2.40 ± 0.1	108 ± 5.50	5.50 ± 0.28	1.30 ± 0.11	33.0 ± 5.0	6.59 ± 0.60	7.93 ± 0.72	4.59 ± 0.45
14-PTA-R035	464	0.8	0.035 ± 0.010	1.8 ± 0.1	46 ± 4	5.6 ± 0.3	0.4 ± 0.1	28.5 ± 0.7	8.7 ± 1.8	9.8 ± 0.6	n/a
14-PTA-R036	465	1.8	0.035 ± 0.010	2.7 ± 0.1	70 ± 4	3.7 ± 0.2	0.3 ± 0.1	452.9 ± 69.4	114.9 ± 29.2	129.5 ± 21.2	n/a
16-PTA-052	426	140	0.021 ± 0.010	2.9 ± 0.1	80 ± 5	20.6 ± 0.5	1.3 ± 0.1	120.8 ± 10.8	21.6 ± 3.6	35.0 ± 4.0	15.5 ± 2.7 (20.5 ± 3.5)

[1] Water contents are "as collected" values and are defined as (mass water)/(mass minerals).

[2] Fading corrections were applied using the method of Huntley and Lamothe (2001). Because the natural signal (Ln/Tn) falls in the non-linear part of the dose response curves of samples, this correction method may underestimate the true age by ~15-20% (e.g., Mathewes et al. 2015).

[3] MAM age in brackets excludes two lowest outlying D_e values.

Appendix A

Appendix A- Published results from the Surficial mapping & geochemistry- Core Zone project

Year	Publication	Description	DOI
2014	OF 7705	Report of Activities for Core Zone 2014: surficial geology, geochemistry, bedrock mapping	10.4095/295521
2015	OF 7946	Report of Activities for Core Zone 2015: surficial geology, geochemistry, gamma-ray spectrometry	10.4095/297388
2016	OF 7967	Till matrix geochemistry results from samples collected in 2014	10.4095/297796
2016	OF 7968	Indicator mineral results from samples collected in 2014	10.4095/297379
2016	OF 8148	Report of Activities for Core Zone 2016: surficial geology, geochemistry, bedrock mapping	10.4095/299295
2017	OF 8187	Indicator mineral results from samples collected in 2015	10.4095/299683
2017	CGM 333	Surficial geology map of NTS 23P northwest	10.4095/306166
2017	OF 8331	Report of Activities for Core Zone 2017: surficial geology, geochemistry, gamma-ray spectrometry	10.4095/306137
2017	OF 8219	Till matrix geochemistry results from samples collected in 2015 and 2016	10.4095/304280
2017	CGM 315	Surficial geology map of NTS 23I southeast	10.4095/300685
2017	CGM 316	Surficial geology map of NTS 23P northeast	10.4095/300656
2017	OF 8222	Gold grains from till samples collected in Core Zone, potential for undiscovered mineralization	10.4095/300657
2017	NL DNR CR 17:119-134	Quaternary mapping and till-geochemistry in western Labrador	ESS Cont. # 20160333
2018	CGM 346	Surficial geology map of NTS 21I southwest	10.4095/306431
2018	OF 8337	Radiometric data for NTS 23-I and 23-P	10.4095/308209
2019	JQS, 34:1-17	Ice flow chronology and subglacial conditions across 23P north, with constraints on deglaciation	10.1002/jqs.3138
2019	CGM 395	Surficial geology map of NTS 23I northeast	10.4095/313655
2019	CGM 377	Surficial geology map of NTS 23I northwest	10.4095/313547
2020	OF 8655	Field data for till samples collected in 2014, 2015, and 2016	10.4095/321471
2020	OF 8721	Clast lithology data for till samples collected in 2014, 2015, and 2016	10.4095/326083
2020	CGM 410	Surficial geology map of NTS 23P southwest	10.4095/14756